

1 **Genome-wide patterns of copy number variation in the**
2 **diversified chicken genomes using next-generation**
3 **sequencing**

4
5 Guoqiang Yi*, Lujiang Qu*, Jianfeng Liu, Yiyuan Yan, Guiyun Xu, and Ning Yang[§]
6

7 Department of Animal Genetics and Breeding, College of Animal Science and
8 Technology, China Agricultural University, Beijing, China

9 *These authors contributed equally to this work

10 [§]Corresponding author:

11 Ning Yang, Ph.D.
12 Department of Animal Genetics and Breeding
13 College of Animal Science and Technology
14 China Agricultural University
15 Beijing 100193, China
16 Tel: +86-10-6273 1351
17 Fax: +86-10-6273 2741
18 E-mail: nyang@cau.edu.cn

19

20 **Manuscript type:** Resource

21

22 **Running title:** Copy number variation in 12 diversified chickens

23

24 **Keywords:** Copy number variation, Whole genome sequencing, aCGH, Genetic
25 diversity, Chicken

26 **Abstract**

27 Copy number variation (CNV) is important and widespread in the genome, and is a
28 major cause of disease and phenotypic diversity. Herein, we perform genome-wide
29 CNV analysis in 12 diversified chicken genomes based on whole genome sequencing.
30 A total of 9,025 CNV regions (CNVRs) covering 100.1 Mb and representing 9.6% of
31 the chicken genome are identified, ranging in size from 1.1 to 268.8 kb with an
32 average of 11.1 kb. Sequencing-based predictions are confirmed at high validation
33 rate by two independent approaches, including array comparative genomic
34 hybridization (aCGH) and quantitative PCR (qPCR). The Pearson's correlation values
35 between sequencing and aCGH results range from 0.395 to 0.740, and qPCR
36 experiments reveal a positive validation rate of 91.71% and a false negative rate of
37 22.43%. In total, 2,188 predicted CNVRs (24.2%) span 2,182 RefSeq genes (36.8%)
38 associated with specific biological functions. Besides two previously accepted copy
39 number variable genes *EDN3* and *PRLR*, we also find some promising genes with
40 potential in phenotypic variants. *FZD6* and *LIMSI*, two genes related to diseases
41 susceptibility and resistance are covered by CNVRs. Highly duplicated *SOCS2* may
42 lead to higher bone mineral density. Entire or partial duplication of some genes like
43 *POPDC3* and *LBFABP* may have great economic importance in poultry breeding. Our
44 results based on extensive genetic diversity provide the first individualized chicken
45 CNV map and genome-wide gene copy number estimates and warrant future CNV
46 association studies for important traits of chickens.

47 **Introduction**

48 Copy number variation (CNV) is defined as gains or deletions of DNA fragments of
49 50 bp or longer in length in comparison with reference genome (Redon et al. 2006;
50 Bickhart et al. 2012). CNVs contribute significantly to both disease susceptibility and
51 resistance and normal phenotypic variability in humans (McCarroll and Altshuler
52 2007; Zhang et al. 2009; Altshuler et al. 2010) and animals (Liu et al. 2010; Yalcin et
53 al. 2011; Wang et al. 2012a; Wang et al. 2012b). Four major mechanisms have been
54 found to be related to CNV formation including non-allelic homologous
55 recombination (NAHR), non-homologous end joining (NHEJ), Fork Stalling and
56 Template Switching (FoSTeS) and LINE1 Retrotransposition (Hastings et al. 2009;
57 Zhang et al. 2009). Additionally, segmental duplications (SDs) which are duplicated
58 sequences (insertions) of ≥ 1 kb in length and $\geq 90\%$ sequence identity are also
59 suggested to be a major catalyst and hotspot for CNV formation (Sharp et al. 2005;
60 Alkan et al. 2009), mainly because regions flanking by SDs are susceptible to
61 recurrent rearrangement by NAHR (Sharp et al. 2005; Freeman et al. 2006). In terms
62 of total bases involved, the percentage of the genome affected by CNVs is higher than
63 that of single nucleotide polymorphism (SNP) markers. Although SNPs are generally
64 considered as suitable markers in the genome-wide association studies (GWAS), most
65 reported SNP variants have relatively limited effects and explain only a small
66 proportion of phenotypic variance (Manolio et al. 2009). Further, CNVs
67 encompassing part or all of a gene or regulatory elements are believed to have
68 potentially larger effects by influencing gene expression indirectly through changing

69 gene structure and dosage, altering gene regulation, exposing recessive alleles and
70 other mechanisms (Redon et al. 2006; Zhang et al. 2009; Conrad et al. 2010; Liu and
71 Bickhart 2012). CNVs are also found to alone capture 18% to 30% of the total
72 detected genetic variation in gene expression in humans and animals, and might
73 contribute to a fraction of the missing heritability (Stranger et al. 2007; Henrichsen et
74 al. 2009). Therefore, identification of CNVs is essential in whole genome
75 fine-mapping of CNVs and association studies for important phenotypes.

76 Originally, two cost-effective and high-throughput methods including array
77 comparative genomic hybridization (aCGH) and commercial SNP microarrays are
78 used for CNV screening (LaFramboise 2009; Pinto et al. 2011). However, different
79 analytic platforms and tools reveal inconsonant results with minimal overlap owing to
80 different designs and genome coverage or density of probes (Henrichsen et al. 2009;
81 Pinto et al. 2011). Due to the limitation in resolution and sensibility, it is difficult for
82 the two approaches to detect small CNVs shorter than 1 kb in length and identify the
83 precise breakpoints of CNVs (Bentley et al. 2008; Yoon et al. 2009). Furthermore, the
84 presence of SD regions is a common challenge for the two platforms, because they are
85 often affected by low probe density and cross-hybridization of repetitive sequence
86 (Campbell et al. 2011; Bickhart et al. 2012). Recently, a variety of CNV detection
87 approaches based on next-generation sequencing (NGS) are proposed and offer a
88 promising alternative as they have a higher effective resolution to discover more types
89 and sizes of CNVs (Teo et al. 2012). One effective method is read depth (RD) (also
90 known as depth of coverage (DOC)) with capability of inferring gain or loss of DNA

91 and determining absolute copy number value of each genetic locus, which detects
92 CNVs by analyzing the number of reads that fall in each pre-specified window of a
93 certain size (Abyzov et al. 2011; Szatkiewicz et al. 2013). Hence, the advent of NGS
94 technologies and suitable analytical method promises to systematically identify CNVs
95 at higher resolution and sensitivity.

96 At present, the three aforementioned high-throughput platforms have been applied to
97 livestock genomics for CNV detection, such as sheep (Norris and Whan 2008), horse
98 (Rosengren Pielberg et al. 2008) and cattle (Bickhart et al. 2012), and suggest several
99 CNVs associated with important phenotypes. CNVs in chickens are also found to be
100 the genetic foundation of phenotypic variation. A duplicated sequence close to the
101 first intron of *SOX5* is associated with the chicken pea-comb phenotype (Wright et al.
102 2009) and an inverted duplication containing *EDN3* causes dermal hyperpigmentation
103 (Dorshorst et al. 2011). Partial duplication of the *PRLR* also shows to be related to the
104 late feathering (Elferink et al. 2008).

105 A genome-wide chicken CNV analysis is essential since the chicken is not only an
106 economically important farm animal but also a valuable biomedical model (Wang et
107 al. 2012b; Jia et al. 2013). However, previous CNV studies in chickens based on
108 aCGH and SNP platforms mainly suffered from low resolution and sensitivity (Griffin
109 et al. 2008; Wang et al. 2012b; Crooijmans et al. 2013; Jia et al. 2013; Tian et al.
110 2013), and a latest report exhibited the detection of four main types of genetic
111 variation from whole genome sequencing data using two chickens (Fan et al. 2013),
112 which suggested the efficiency of CNV detection via deep sequencing. To construct a

113 more refined and individualized chicken CNV map and investigate genome-wide
114 CNV genotyping, benefiting from extensive genetic diversity in Chinese indigenous
115 (Qu et al. 2006) and commercial chickens, we describe the use of NGS data to detect
116 CNVs in the diversified chicken genomes, and estimate genome-wide gene copy
117 number, enabling us to better understand the patterns of CNVs in the chicken genome
118 and future CNV association studies similar to SNPs.

119 **Results**

120 **Mapping statistics and CNV detection**

121 We performed whole genome sequencing in 12 different breeds of female chickens
122 using Illumina paired-end library and obtained a total of 12.9 Gb of high quality
123 sequence data per individual after quality filtering. After sequence alignment and
124 removing potential PCR duplicates, the sequence depth for each individual varied
125 from 8.2× (CS) to 12.4× (WR), which was sufficient for CNV detection, and the
126 average coverage with respect to the chicken genome reference sequence was 97.2%
127 (**Table 1**). We calculated the average RD for 5 kb non-overlapping windows for all
128 autosomes and performed GC correction as previous reports. The GC-adjusted RD
129 mean and standard deviation (STDEV) of autosomes for each individual was listed in
130 **Table 1**. We applied the program CNVnator to 12 individuals and the average number
131 of CNVs per individual was 1,389, ranging from 703 in WL to 1,975 CNVs in BY. A
132 detailed description of CNV calls could be found in **Supplementary Table S1**. The
133 mean CNV size in BY (17.4 kb) and CS (14.7 kb) was significantly larger than that of
134 the other individuals (from 4.7 kb in WR to 8.5 kb in SK). In addition, the proportion

135 of CNVs less than 10 kb in length was smaller in BY (52.6%) and CS (54.8%)
136 compared with others (from 73.4% in SK to 90.3% in WR). For all CNVs classified
137 as duplication, the autosomal maximum copy number was 40.8 on chromosome 2
138 (chr2) in RJF, and the average copy number of all duplicated regions on autosomes in
139 all individuals was 3.88.

140 A total of 9,025 CNV regions (CNVRs) allowing for CNV overlaps of 1 bp or greater
141 were obtained, mainly on the 28 autosomes, two linkage groups and sex chromosomes,
142 which amounted to 100.1 Mb of the chicken genome and corresponded to 9.6% of the
143 genome sequence. The individualized chicken CNV map across the genome was
144 shown in **Supplementary Figure S1**. The length of CNVRs ranged from 1.1 to 268.8
145 kb with an average of 11.1 kb and a median of 6.6 kb. In total, 6,276 (69.5%) out of
146 all CNVRs had size varying from 1.1 to 10 kb (**Figure 1a**). Although chr1 had a
147 maximum of 1,933 CNVRs, the two largest CNVR density, defined as the average
148 distance between CNVRs, were 35.7 kb and 32.0 kb on the chr16 and LGE64
149 respectively (**Supplementary Table S2**). Meanwhile, Among all CNVRs, 6,160
150 (68.3%) were present in a single individual, 1,461 (16.2%) were shared in two
151 individuals and 1,404 (15.5%) shared in at least three individuals (**Figure 1b**). Further,
152 the mean and median of the specific CNVRs was 8.9 kb and 5.8 kb in size, whereas
153 the shared CNVRs size was 15.9 kb in average and 9.5 kb as the median. According
154 to the type of CNVRs, they were divided into three categories, including 4,821 gain,
155 3,854 loss and 350 both (gain and loss) CNVRs. The number of CNVRs in different
156 individuals varied greatly, ranging from 677 in WL to 1,933 in BY, and was positively

157 related to the proportion of specific CNVRs in an individual. BY and CS had the
158 greatest CNVR diversity, with 835 and 820 unique CNVRs amounting to 13.8 Mb and
159 13.6 Mb respectively, as compared to 152 and 174 unique CNVRs comprising 0.6 Mb
160 and 0.7 Mb in WL and WR. In addition, 160 CNVRs located on chrUn covered 1.5
161 Mb of genome sequence and may be copy number variable between individuals.
162 Although we employed stringent quality control for those regions, candidate CNVRs
163 on chrUn were worth a thorough study owing to the shorter length of the chrUn
164 contigs and mapping ambiguity of chrUn sequence reads.

165 **Experimental validation**

166 The copy number value of diploid regions in autosomes theoretically equals to two, so
167 we could test the potential for CNVnator to generate false positive results by
168 evaluating these two copies regions. For all 12 individuals, we selected all 5 kb
169 non-overlapping windows in autosomes and excluded all windows intersecting with
170 predicted CNVs and gaps, and then estimated their average CN. The average CN and
171 STDEV per individual was 2.077 ± 0.291 , varied from 2.041 ± 0.226 in WR to $2.104 \pm$
172 0.299 in RJF, showing low variability within the predicted neutral regions. Further, to
173 validate sequencing-based CNV predictions, we carried out two independent
174 experiments including aCGH and qPCR as two traditional CNV detection approaches
175 to compare with computational predictions. We performed 11 pairwise aCGH
176 experiments using RJF as the reference for all experiments and all others as test
177 samples. Considering that we estimated CN of selected individuals with respect to
178 reference genome which cannot be used for the aCGH reference sample, we

179 calculated the predicted \log_2 CN ratios for the 11 aforementioned individuals against
180 RJF based on computational copy number estimates to make the CN values
181 comparable with the aCGH results, which was designated as digital aCGH approach
182 (Sudmant et al. 2010). We first split the predicted overlapping CNVs from test
183 samples and RJF into non-overlapping segments and estimated CN of each segment
184 for each of the two samples, and divided the segment CN of test sample by RJF and
185 calculated \log_2 CN ratios as digital aCGH values. Then we compared the digital
186 values with aCGH probe \log_2 ratios which were defined as the average of all probes
187 \log_2 ratio values in corresponding segments. We performed a simple linear regression
188 analysis to explain the correlation between two values. Pearson correlation values (r)
189 ranged from 0.395 in SK to 0.740 in LX among all 11 individuals (**Figure 2** and
190 **Supplementary Figure S2**), and eight of which were greater than 0.600. BY (0.459),
191 SK (0.395) and WR (0.477) showed lower correlation less than 0.500 compared with
192 other individuals larger than 0.600, we found the mean of all probes \log_2 ratio values
193 in the three aforementioned individuals were 1.05, 0.85 and 1.05 respectively, and
194 were larger than the value of others which were close to zero.

195 In addition, we chose to investigate 15 predicted CNVRs representing different types
196 and frequencies, and tested all 12 samples for each CNVR. Two distinct pairs of
197 primers were designed for each predicted CNVR (**Supplementary Table S3**). The
198 proportions of confirmed positive samples (positive predictive value) varied from 50%
199 to 100%, with an average of 91.71%. However, some negative samples were also
200 confirmed to contain CNV, and the false negative rate varied from 0 to 60%, with an

201 average of 22.43%. We illustrated the qPCR results for three confirmed CNVRs of
202 different types (gain, loss and both) (**Supplementary Figure S3**).

203 **Copy number polymorphic genes**

204 We obtained 5,924 non-redundant RefSeq gene transcripts retrieved from the UCSC
205 Genome browser and identified copy number polymorphic genes in different
206 individuals through estimating the copy number of each gene by CNVnator. A total of
207 2,182 genes (36.8%) overlapped with 2,188 predicted CNVRs (24.2%), while the
208 other 3,742 (63.2%) did not. Among them, 535 genes were found to be completely
209 overlapped by CNVRs. The overlapping genes were found not to be highly duplicated
210 sequences, and the maximum copy number is 12.0. We focused on the genes on the
211 anchored chromosomes for the further analysis and discussion due to their clear
212 chromosome locations. We identified the 25 most variable genes according to the
213 STDEV of each gene CN in different individuals, and found that these genes were
214 mainly involved in immune response and keratin formation (**Table 2** and
215 **Supplementary Table S4**). The number of genes intersecting with putative CNVs in
216 different individuals varied greatly, ranging from 154 in WR to 780 in BY, and only
217 nine genes were shared by all surveyed individuals. Keratin gene families were
218 detected to have large CN values and variances. Two significant CNVRs associated
219 with dermal hyperpigmentation were located on chr20 at positions 11,217,001 to
220 11,272,200 (CNVR7984) and 11,651,801 to 11,822,900 (CNVR7990), which had
221 already been described in detail in previous study (Dorshorst et al. 2011), and the
222 distance between two loci was 379.6 kb. *SLMO2* and *TUBB1* as the candidate genes

223 were completely covered by the first region which was predicted about twice as many
224 copies of the region in DX and SK as in other individuals (**Figure 4a and**
225 **Supplementary Figure S4a**). The major functional gene *EDN3* (endothelin 3) is not
226 archived because predicted gene is not available for UCSC RefSeq database. We
227 found that only BY had this CNVR while SK and DX as two typical breeds with
228 dermal hyperpigmentation did not. So we further checked the raw results before
229 removing CNVs overlapping with gaps. Two nearly identical CNVs were found, one
230 at positions 11,111,501 to 11,238,600 in DX and the other at positions 11,111,401 to
231 11,238,900 in SK comprising two gaps larger than 100 bp, which were also confirmed
232 by our whole genome aCGH (**Figure 4a and Supplementary Figure S4a**). The
233 distance between the raw CNVR and the second region (CNVR7990) is 412.9 kb and
234 almost perfectly supports the reported results (Dorshorst et al. 2011). Conversely, the
235 first CNVR in BY (11,217,001 to 11,272,200) showing normal skin color does not
236 contain *EDN3* gene (11,148,025 to 11,160,484), also provides evidence that copy
237 number variable *EDN3* is the causal mutation resulting in dermal hyperpigmentation.
238 Another previously identified CNVR involving *PRLR* (prolactin receptor) gene on
239 chrZ (Elferink et al. 2008) was also detected in our study in which the CN of *PRLR* in
240 WC and WL are twice as many as in other individuals. The sex-linked *K* allele
241 containing two copies of *PRLR* in females is associated with late feathering and used
242 widely for sexing hatchlings. Our sequencing-based and qPCR results showed that
243 WC and WL should exhibit the late feathering phenotype, which is supported by
244 actual phenotype record.

245 In addition, we found some genes related to the host immune and inflammatory
246 response. For example, *CD8A*, *FZD6*, *LIMS1*, *TNFSF13B* and some MHC genes
247 associated with Marek's disease (MD) were found to have CNVR overlaps, and the
248 same case with genes for avian resistance to bacteria, such as *CDH13* and *CALM1*.
249 *SOCS2* involving in the regulation of bone growth and density was predicted to have
250 the largest CN values in LX (n = 6.4), while DX (n = 3.0) and TB (n = 3.6) also
251 showed the duplicated sequence compared with the neutral of the other individuals in
252 the loci (**Figure 4b and Supplementary Figure S4b**). LX represents a characteristic
253 breed for cockfighting in which bone strength is an essential feature for selection. To
254 validate the highly duplicated sequence (CNVR412) found only in LX, we selected
255 another 16 individuals, *i.e.*, eight LX (four males and four females) and other eight
256 females consisting of one CS, one DX, one SG, one SK, two TB and two WL, to
257 perform qPCR experiments using the same two pairs of primers listed in
258 **Supplementary Table S3**. Two qPCR results demonstrated copy number estimate of
259 almost each LX was larger than others (**Figure 3**), and the average copy number (5.0
260 and 5.2 for two pairs of primers, respectively) of all LX were significant larger than
261 those (2.6 and 2.6) in other individuals using the two-sample t-test (P -value = 0.003
262 and 0.001). Additionally, other identified CNV-gene overlaps were detected to be
263 potentially responsible for economic traits, as these genes were involved in lipid
264 metabolism, muscle development and growth, and secretion process containing
265 hormone, protein and biotin. For example, our results suggested higher copy number
266 for the *POPDC3* gene in WL (n = 4.2) than in the other 11 genomes (n = 2.3) (**Figure**

267 **4c and Supplementary Figure S4c**). Similarly, the WL genome showed the greatest
268 number of *AVR2* copies ($n = 2.0$) on chrZ compared with others ($n = 1.1$). Two
269 promising genes involving in lipid metabolism, *AP2MI* and *LBFABP*, were identified
270 as the largest copy number ($n = 3.0$ and 3.2) in meat-type chicken (CS) compared
271 with those of all others.

272 **Heatmap analysis**

273 We performed a hierarchical clustering heatmap analysis and generated heatmaps
274 based on Pearson's correlation using the CN values for selected gene loci, in order to
275 infer the potential evolutionary history of some genes among 12 individuals. Two
276 genes *SLMO2* and *TUBB1* in DX and SK, were found to be highly duplicated regions
277 and the two individuals were clustered into one group (**Figure 5a**). Another promising
278 gene *SOCS2* was also confirmed for the difference in copy number between LX and
279 others (**Figure 5b**). Meanwhile, WL showed specific expansion in *POPDC3* locus
280 and was split into a separate clade (**Figure 5c**).

281 **Gene content and QTL analysis of CNVRs**

282 A total of 2,182 RefSeq genes overlapped putative CNVRs. Then, we performed gene
283 ontology (GO) and Kyoto Encyclopedia of Genes and Genomes (KEGG) pathway
284 analysis for these variable genes. The GO analysis revealed 641 GO terms, of which
285 157 were statistically significant after Benjamini correction (**Supplementary Table**
286 **S5**). And GO terms showing significant enrichment were mainly involved in positive
287 regulation of macromolecule metabolic process and gene expression, plasma
288 membrane, protein localization, enzyme binding, response to oxidative stress and

289 immune system development. The KEGG pathway analysis indicated that the variable
290 genes were overrepresented in 11 pathways, but none of which was significant after
291 Benjamini correction. According to our artificial QTL filtering criteria, we identified
292 595 high-confidence QTLs in total, of which 301 (50.6%) were found to overlap with
293 561 CNVRs (6.2%) (**Supplementary Table S6**). These QTLs were mainly involved
294 in production and health traits, such as growth, body weight, abdominal fat weight,
295 egg number and Marek's disease-related traits.

296 **Discussion**

297 This study performed genome-wide CNV detection, estimated absolute copy number
298 values and constructed the first individualized chicken CNV map using NGS
299 technology and RD method, which has advantages in both technology platform and
300 genetic diversity compared with previous reports (Wang et al. 2012b; Crooijmans et al.
301 2013; Fan et al. 2013; Jia et al. 2013). CNV constitutes a major source of genetic
302 variation that is complementary to SNP and could account for a substantial part of
303 missing heritability (Manolio et al. 2009), because a significant fraction of CNVs fall
304 in genomic regions not well covered by SNP arrays, especially SD regions lacking of
305 sufficient probes (Campbell et al. 2011; Liu and Bickhart 2012). Most CNV studies to
306 date have been discovery studies rather than association studies, mainly due to the
307 limitations of CNV resolution and genotyping in each individual (McCarroll and
308 Altshuler 2007). The high-resolution individualized chicken CNV map based on
309 extensive genetic diversity not only enriches genetic variation database but also
310 encourages the future development of assays for accurately genotyping CNVs,

311 enabling systematic exploration about CNV association studies similar to SNPs. In
312 future, integration of CNVs with SNPs may be an effective and promising way to
313 elucidate the causes of complex diseases and traits (Stranger et al. 2007; Liu and
314 Bickhart 2012).

315 The average number of putative CNVs per individual is 10 to 30 times more than that
316 detected by previous aCGH studies (40 and 103 CNVs per individual; (Wang et al.
317 2012b; Crooijmans et al. 2013)) and four times more than our high-density aCGH
318 results (391 CNVs per individual), and about 75% CNVs are smaller than 10 kb. It is
319 mainly because most CNVs in genome are less than 10 kb in size, aCGH platforms
320 with insufficient probes density have the limited capability of detecting them, whereas
321 RD analysis is able to discover CNVs with a few hundred bases by increasing
322 sequencing coverage (Abyzov et al. 2011). Additionally, the number of CNV events
323 per individual in a recent report (4,419 CNVs; (Fan et al. 2013)) is larger than that in
324 our results, owing to the difference between two CNV detection algorithms and
325 post-filtering methods.

326 The number of CNVs and CNVRs even genes overlapping with CNVs in each
327 individual varies greatly, and all individuals shares a small number of those, likely
328 due to the distant relationship between 12 breeds for various breeding objectives. Out
329 of all CNVRs, the percentage of CNVRs called in a single chicken breed is 68.3% and
330 is similar to the other studies in chicken (71%, 73%, 64% and 62%; (Wang et al. 2010;
331 Wang et al. 2012b; Luo et al. 2013; Tian et al. 2013)), while significantly higher than
332 in human (49%; (Conrad et al. 2010)), cattle (32%; (Bickhart et al. 2012)) and dog

333 (21%; (Berglund et al. 2012)). Because recombination rate is much higher in the
334 chicken genome (2.5-21 cM/Mb) compared with some mammalian such as human (1
335 cM/Mb) and mouse (0.5 cM/Mb) (Wong et al. 2004), and recombination-based
336 mechanisms such as non-allelic homologous recombination (NAHR) are the major
337 causes leading to CNVs (Munoz-Amatriain et al. 2013), we speculate that these
338 specific CNVRs for a breed may be recent events and contribute to breed-specific
339 phenotype and performance, and other CNVRs shared across breeds suggest their
340 relative ancient origin or neutral evolutionary histories and seem to be fixed in all
341 breeds. Meanwhile, the breed-specific CNVRs have smaller mean size because recent
342 large scale variations may cause dysfunction and even be lethal (Conrad et al. 2006).
343 Owing to only one individual per breed, a larger sample especially biological
344 replicates within breed is crucial for validation study.

345 We find both maximum and mean copy number of duplicated sequences in chicken
346 are less than those in mammals (Alkan et al. 2009; Bickhart et al. 2012), which
347 may be related to the relatively smaller genome size (only one third of a typical
348 mammalian genome) and the lower repetitive DNA content in the chicken (Burt 2005).

349 In addition, the covered sequence of gain CNVRs is larger than that of loss CNVRs
350 because chromosomal deletion can lead to a variety of serious malformations and
351 disorders and is subjected to purifying selection (Conrad et al. 2006; Freeman et al.
352 2006). In general, the length of chromosome is positively correlated with the number
353 of CNVRs. The chr16 (a microchromosome) is found to have the second densest
354 CNVRs, possibly owing to the highly variable major histocompatibility complex

355 (MHC) regions and higher recombination rate, which result in the most genetic
356 diversity of any chromosome (International Chicken Genome Sequencing Consortium
357 2004).

358 It is generally believed that the CN of neutral regions is between 1.5 and 2.5 (Abyzov
359 et al. 2011) and the $\text{mean} \pm 2 \times \text{STDEV}$ in our results corresponds closely to the theory,
360 which demonstrates that CNVnator has efficient performance on CNV detection and
361 CN estimation and can generate most reliable results. In addition, two independent
362 validation experiments also suggest excellent accuracy and reliability of our predicted
363 results. We first compare RD predicted CNVs with aCGH results, and the positive
364 correlation between computational and experimental \log_2 CN ratios in our study is
365 higher than the previous result (Bickhart et al. 2012), due to the two aCGH platforms
366 with higher resolution for our analysis. The low correlation coefficients in BY, SK and
367 WR may disclose certain experimental noises and biases resulting in misgenotyping
368 in corresponding aCGH experiments (Liu and Bickhart 2012), particularly
369 high-frequency duplications and rare deletions (Conrad et al. 2010; Abyzov et al.
370 2011). We then perform quantitative PCR for 15 randomly chosen CNVRs. The
371 average of positive predicted value of the 15 validated CNVRs was 91.71%, similar to
372 the results of previous reports in animals (Wang et al. 2012a; Jiang et al. 2013; Tian et
373 al. 2013), suggesting that most of positive samples detected by sequencing-based are
374 highly consistent with the qPCR experiments. Whereas we also estimate the false
375 negative error rates as it is a common problem in CNV detection (Nicholas et al. 2009;
376 Wang et al. 2012a), the average percentage of false negative results for each CNVR is

377 22.43%. This result may be due to the fact that we apply stringent criteria of CNV
378 detection in order to minimize the false positive rate, while it also simultaneously
379 results in possible increase in false negative rate.

380 Our results showed that 36.8% RefSeq genes intersected with 24.2% predicted
381 CNVRs. It is probable that CNVs are located preferably in gene-poor regions (gene
382 deserts and devoid of known regulatory elements), especially deletions (Conrad et al.
383 2006; Freeman et al. 2006), because gene-rich CNVs are more likely to be pathogenic
384 than gene-poor CNVs and these deleterious CNVs are removed by purifying selection
385 (Conrad et al. 2006; Lee et al. 2007). Meanwhile, the maximum CN of all genes
386 overlapping with CNVs is 12.0, suggesting again that chicken genome has lower
387 repetitive DNA content (Burt 2005). It is noted that some highly duplicated genes,
388 especially nine out of the 25 most variable genes, belong to four keratin subfamilies
389 (claw, feather, feather-like and scale) in chicken. In birds, skin appendages such as
390 claws, scales, beaks and feathers are composed of beta (β) keratins and can prevent
391 water loss and provide a barrier between the organism and its environment
392 (Greenwold and Sawyer 2010), and the avian keratin genes are significant
393 over-represented with respect to mammals (International Chicken Genome
394 Sequencing Consortium 2004; Crooijmans et al. 2013). High CN keratin genes
395 suggest the scenario for the evolution of the β -keratin gene family through gene
396 duplication and divergence for their adaptive benefits (Zhang et al. 2009; Greenwold
397 and Sawyer 2010). Additionally, the four subfamilies of β -keratin genes form a cluster
398 on chr25 which is one of the more GC-rich chromosomes and contains a relatively

399 larger number of minisatellites (Greenwold and Sawyer 2010), which also result in
400 high copy number of genes.

401 CNV is a significant source of genetic variation accounting for disease and
402 phenotypic diversity, due to the duplication or deletion of covered genes or regulation
403 elements (Zhang et al. 2009), which are major forces of evolutionary innovation
404 (Wapinski et al. 2007). Hierarchical clustering analysis of animals based on CN
405 content within given locus could bring similar individuals during evolution into the
406 same group and reveal the evolutionary relation shown by the heatmap. For example,
407 a hierarchical clustering of CN values within *SLMO2* and *TUBB1* loci group DX and
408 SK together, and both of which are distributed in the Jiangxi province of China,
409 suggesting that DX and SK may have a close evolutionary relationship evolving from
410 a common ancestor or purposely bred dermal hyperpigmentation into different strains.

411 We detected CN differences for several interesting genes related to specific
412 phenotypes among the surveyed individuals. For example, the *SOCS2* (suppressor of
413 cytokine signaling 2) is a member of the suppressor of cytokine signaling family, the
414 related proteins are implicated in the negative regulation of cytokine action through
415 inhibition of the JAK/STAT pathway (Janus kinase/signal transducers and activators
416 of transcription) (Metcalf et al. 2000). Dual x-ray absorptiometry (DXA) analysis
417 demonstrated that *SOCS2* inactivation resulted in reduced trabecular and cortical
418 volumetric bone mineral density (BMD) in *SOCS2*-deficient mice (Lorentzon et al.
419 2005). We find that *SOCS2* has the highest CN (n = 6.4) in LX than in the other
420 individuals, which is particularly interesting as the LX is known for the cockfighting

421 in which chickens with higher BMD have advantage over others. The gene
422 expansions are also supported by heatmap. Additional qPCR experiments in other 16
423 individuals reveal that the increased copy number of *SOCS2* in LX is larger than
424 others. We suspect that the copy number polymorphic locus is almost ubiquitous in
425 chickens, but the particularly high gene duplication in LX may be as a result of the
426 genetic effect of long-term artificial selection such as crossing between individuals
427 with stronger bone.

428 Additionally, both the copy number estimates of *POPDC3* (popeye domain containing
429 3) and *AVR2* (avidin related protein 2) in WL were found to be about twice as many
430 copies as other individuals. We draw a heatmap for *POPDC3* in WL to visualize
431 specific gene duplication and clustering feature. The *POPDC3* gene belongs to
432 Popeye family encoding proteins with three potential transmembrane domains with a
433 high degree of sequence conservation, and is preferentially expressed in heart and
434 skeletal muscle cells as well as smooth muscle cells (Brand 2005). It had been
435 reported that the expression of two Popeye family members was upregulated in uterus
436 of pregnant mice (Andree et al. 2000). Uterus has been thought to be an organ
437 composed of smooth muscle and containing the shell gland in favor of depositing
438 eggshell (Hincke et al. 2012), and duplication in *POPDC3* gene may facilitate
439 myometrium maturation and labor as well as uterine fluid secretion during the egg
440 laying period. Of the *AVR2* gene products, avidin is known to be the operational
441 biotin-harvester produced in the oviducts of birds and deposited in the avian
442 egg-white, comprising approximately 0.05% of the total protein in chicken egg-white.

443 The function of *AVR2* has been postulated to be implicated in inflammation response
444 in the manner of an antibiotic (Hytonen et al. 2005). WL is the most prolific egg
445 laying chicken due to the fact that it has been extensively bred for egg production,
446 thus the oviduct and uterus, serving as two important parts of the reproductive organs,
447 are always in highly active state, and copy number increase at these loci related to
448 laying may reveal important differences in abilities like protein secretion and eggshell
449 formation between WL and other breeds.

450 Meat production is also a trait of economic importance. CS is a commonly used breed
451 in the chicken meat industry and is found to have the largest CN of the *AP2M1*
452 (adaptor-related protein complex 2, mu 1 subunit) and *LBFABP* (liver basic fatty acid
453 binding protein) genes which are related to lipid metabolism and transport. *AP2M1*
454 has been shown in microarray experiments to have higher expression in persons who
455 fail to control their weight after weight reduction (Marquez-Quinones et al. 2010).
456 Moreover, *LBFABP* is a member of the fatty acid-binding proteins (FABPs) family
457 and expressed only in the liver playing a major role in lipid metabolism. It had been
458 reported that feeding simulation was the primary factor increasing the expression of
459 *LBFABP* gene (Murai et al. 2009). Duplication of the *AP2M1* and *LBFABP* locus in
460 CS could potentially increase their expression, and may be associated with fatty acid
461 utilization and weight gain.

462 Our findings suggest that many potential CNV-gene overlaps, like *CD8A*, *BF2* and
463 *CALM1*, are associated with diseases susceptibility and resistance (Liaw et al. 2007;
464 Goto et al. 2009; Connell et al. 2013), and also prove the two previous copy number

465 variable genes involving in MD disease, namely *FZD6* (frizzled family receptor 6)
466 and *LIMS1* (LIM and senescent cell antigen-like domains 1) (Wang-Rodriguez et al.
467 2002; Chen et al. 2008; Luo et al. 2013). Genes intersecting with CNVRs may be
468 important sources of disease and phenotypic diversity through reshaping gene
469 structure and modulating gene expression (Zhang et al. 2009). Moreover, these
470 enriched GO terms are involved in cellular regulation and structure as well as various
471 binding functions, in which most genes may be haploinsufficient, and duplication of
472 them could improve fitness through selection on increased dosage effects (Nguyen et
473 al. 2006). It is notable that several GO terms related to stress and immune response
474 are overrepresented, suggesting that the CN variable genes may influence the
475 responses to environmental stimuli and provide the mutational flexibility to adapt
476 rapidly to changing selective pressures due to the signatures of adaptive evolution
477 (Gokcumen et al. 2011).

478 **Conclusions**

479 In this study, we performed genome-wide CNV detection and absolute copy number
480 estimates of corresponding genetic locus based on the whole genome sequencing data
481 of 12 chickens abundant in genetic diversity, and constructed the highest-resolution
482 individualized chicken CNV map so far. We identified a total of 9,025 CNVRs in all
483 individuals. Validation of CNVRs by aCGH and qPCR produced a high rate of
484 confirmation, suggesting sequencing-based method was more sensitive and efficient
485 for CNV discovery and genotyping. We have detected 2,182 RefSeq genes as copy
486 number variable among 12 individuals, including genes involved in well-known

487 phenotypes such as dermal hyperpigmentation and late feathering. In addition, some
488 novel genes like *POPDC3* and *LBFABP* covered by CNVs may play an important role
489 in production traits, and highly duplicated *SOCS2* may serve as an excellent candidate
490 for bone mineral density. Our study based on extensive genetic diversity lays the
491 foundation for comprehensive understanding of copy number variation in chicken
492 genome and is beneficial to future association studies between CNV and important
493 traits of chickens.

494 **Methods**

495 **Sample collection and sequencing**

496 We selected a total of 12 female chickens from different types and genetic sources
497 representing modern chicken populations with abundant genetic diversity, *i.e.*, a Red
498 Jungle Fowl (RJF, the ancestor of domestic chickens), seven Chinese indigenous
499 chickens including Beijing You (BY), Dongxiang (DX), Luxi Game (LX), Shouguang
500 (SG), Silkie (SK), Tibetan (TB) and Wenchang (WC), and four commercial breeds
501 including Cornish (CS), Rhode Island Red (RIR), White Leghorn (WL) and White
502 Plymouth Rock (WR). The whole blood samples were collected from brachial veins
503 of chickens by standard venepuncture along with regular quarantine inspection of the
504 experimental station of China Agricultural University, and genomic DNA was isolated
505 using standard phenol/chloroform extraction method. Whole genome sequencing for
506 all 12 individuals was performed on the HiSeq 2000 system (Illumina Inc., San Diego,
507 CA, USA). Two genomic DNA libraries of 500 bp insert size per individual were
508 constructed and sequenced with 100 bp paired-end reads, and each library dataset was

509 generated with a five-fold coverage depth. Library preparation and all Illumina runs
510 were performed as the standard manufacturer's protocols.

511 **Quality control and Sequence alignment**

512 For ensuring high-quality data, we used NGS QC Toolkit with default parameters to
513 perform quality control of raw sequencing data, mainly by removing low-quality
514 reads and reads containing primer/adaptor contamination (Patel and Jain 2012). All
515 high-quality Illumina sequence reads were aligned against the galGal4 as a reference
516 source by using Burrows-Wheeler Aligner (BWA) program (Li and Durbin 2009) with
517 default parameters. The assembly of the reference genome was retrieved from the
518 UCSC website (<http://hgdownload.soe.ucsc.edu/goldenPath/galGal4/bigZips/>). The
519 BWA aligned output format was set to SAM. During the construction of a genomic
520 library, Illumina platform was likely to generate some duplicate reads named 'PCR
521 and optical duplicates' which imposed significant impact on the downstream analysis.
522 So we first used SAMtools (Li et al. 2009) to convert the .sam files of different
523 libraries belonging to the same individual to .bam files and sort and merge them,
524 followed by removal of potential PCR duplicates using Picard
525 (<http://picard.sourceforge.net/>).

526 **CNV detection**

527 Following the above filtering step, the resulting .bam files were utilized for calling
528 and genotyping of CNVs, post-processing were performed using CNVnator software
529 based on RD method as previously described (Abyzov et al. 2011). CNVnator firstly
530 calculated the count of mapped reads within user specified non-overlapping bins of

531 equal size as the RD signal, and then adjusted the signal in consideration of a
532 correlation of RD signal and GC content of the underlying genomic sequence. The
533 mean-shift algorithm was employed to segment the signal with presumably different
534 underlying CNs. Putative CNVs were predicted by applying statistical significance
535 tests to the segments. A more detailed description of method could be found at
536 CNVnator paper (Abyzov et al. 2011). We ran CNVnator with a bin size of 100 bp for
537 our data. CNV calls were filtered using stringent criteria including a *P*-value < 0.01
538 and a size > 1 kb, and calls with > 50% of q0 (zero mapping quality) reads within the
539 CNV regions were removed (q0 filter), and calls overlapping with gaps which is
540 larger than or equal to 5 bp in the reference genome were excluded from consideration.
541 In unknown chromosomes (chrN_random and chrn_random in UCSC, chrUn), we
542 controlled CNV size to be shorter than arbitrary 1/10 total length of respective contig
543 for reliable CNV detection considering the percentage of CNV versus
544 macrochromosomes in length is approximate to 10% and CNV should be much shorter
545 than a contig. Meanwhile, we performed genotyping of all 5 kb non-overlapping
546 windows which did not overlap with putative CNVs and gaps in autosomes.

547 **aCGH validation**

548 Initially, NimbleGen whole genome tiling array used in our experiment was a
549 custom-designed 3*1.4 M array based on galGal4 2011 build, which contained a total
550 of 1,425,178 50-75mer probes with a mean and median interval of 734 bp and 700 bp.
551 The DNA labeling (Cy3 for samples and Cy5 for references), array hybridization, data
552 normalization and scanning analysis were performed by NimbleGen Systems Inc.

553 (Madison, WI, USA). Image and segmentation analysis were performed using
554 NimbleScan 2.5 (segMNT algorithm) with parameter preset by the manufacturer.
555 However, there was some trouble during the NimbleGen aCGH experiments. Because
556 none of results were obtained in three consecutive trials for CS, RIR and WL and this
557 type of NimbleGen CGH array stopped production subsequently. Considering we only
558 analyzed raw aCGH \log_2 ratio values instead of processed/normalized data, so we
559 chose a similar Agilent custom-designed 1*1.0 M array (Agilent Technology Inc., CA,
560 USA) with the mean and median probe spacing of 1,056bp and 1,050bp, respectively.
561 And all data processing was performed in terms of standard Agilent procedure. In
562 each aCGH experiment, we chose the RJF as the same reference sample.

563 **Quantitative PCR confirmation**

564 We also performed qPCR confirmation of 15 CNVRs chosen from the CNVRs
565 detected by CNVnator. Most chosen CNVRs have not been reported in previous
566 studies and are also adjacent to annotated genes. Two distinct pairs of PCR primers
567 were designed to target each CNV region using Primer5.0 software for the uncertainty
568 in CNVR breakpoints. Furthermore, the UCSC In-Silico PCR tool was used for in
569 silico analysis of primers specificity and sensitivity (Karolchik et al. 2008). *PCCA*
570 which was previously identified as a non-CNV locus was chosen as a control region
571 (Wang et al. 2010). Quality control of all primer sets were evaluated using an 8-point
572 standard curve in duplicate to ensure the similar amplification efficiencies between
573 target and control primers. All qPCR experiments were conducted on an ABI Prism
574 7500 sequence detection system (Applied Biosystems group) using SYBR green

575 chemistry in triplicate reactions, each with a reaction volume of 15 μ l in a 96-well
576 plate. The condition for thermal cycle was as follows: 1 cycle of pre-incubation at 50°C
577 for 2 min and 95°C for 10 min, 40 cycles of amplification (95°C for 10 s and 60°C
578 for 1 min). We used the formula $2^{(1 - \Delta\Delta Ct)}$ method to calculate the relative copy
579 number for each test region by assuming that there were two copies of DNA in the
580 control region. The cycle threshold (Ct) value of each test sample was normalized to
581 the control region first, and then the ΔCt value was calculated between the test sample
582 and a preselected reference sample predicted without CNV by CNVnator. The golden
583 standard of each diploid CNVR was generally considered to have two copies for
584 autosomes or one copy when the locus was on Z chromosome of a female in chickens.

585 **Gene contents and functional annotation**

586 The RefSeq gene list was retrieved from the UCSC RefSeq database (Karolchik et al.
587 2008). All miRNA genes were excluded because the nucleotide sequences were too
588 short to estimate reliable copy number. We analyzed the proportion of the RefSeq
589 genes overlapping with putative CNVRs and performed CN estimates on all 5,927
590 non-redundant RefSeq gene transcripts. In addition, to provide insight into the
591 functional enrichment of the RefSeq genes overlapping with CNVRs, we performed
592 Gene Ontology (GO) functional annotation and Kyoto Encyclopedia of Genes and
593 Genomes (KEGG) pathway analysis employing the web-accessible program DAVID
594 (Huang da et al. 2009) and selecting the DAVID default population background which
595 was appropriate for high-throughput studies in enrichment calculation. Statistical
596 significance was assessed by using P value ($P < 0.05$) of a modified Fisher's exact

597 test and Benjamini correction for multiple testing. We also investigated the CNVRs
598 identified in this study with the reported QTLs obtained from Chicken QTL database
599 (Hu et al. 2013). We focused on the QTLs with confidence interval less than 10 Mb
600 and considered those QTLs with overlapped confidence intervals greater than 50% as
601 the same QTL (Jiang et al. 2013), because the QTL confidence intervals were too
602 large to be used efficiently in post-processing.

603 **Heatmap hierarchical cluster analysis**

604 We used the heatmap.2() function of the gplots package ([http://cran.r-project.org/web/](http://cran.r-project.org/web/packages/gplots/index.html)
605 [packages/gplots/index.html](http://cran.r-project.org/web/packages/gplots/index.html)) to generate heatmap figures. We first selected the
606 specified regions extending 30 kb on each side of interesting genes and used the
607 estimated CN values of 1 kb non-overlapping windows for each animal for post
608 analysis, mainly considering that some regulatory elements may be included in the
609 upstream or downstream of a gene. No reordering of those windows representing
610 corresponding chromosome locations in heatmap was made for the sake of clarity.
611 The Pearson's correlation coefficient (1-r) of the CN values was used as a distance
612 measure of the agglomerative hierarchical clustering with average linkage, and to
613 generate hierarchical cluster dendrograms for each animal.

614 **Data access**

615 All aCGH data have been submitted to the NCBI Gene Expression Omnibus (GEO)
616 (<http://www.ncbi.nlm.nih.gov/geo/>) under accession number GSE54119.

617 **Acknowledgements**

618 We thank Xiquan Zhang for sharing some samples. This work was funded in part by

619 Programs for Changjiang Scholars and Innovative Research in University (IRT1191),
620 and China Agriculture Research Systems (CARS-41).

621 **Authors' contributions**

622 N.Y. and L.Q. conceived and designed all experiments. G.Y., L.Q. and Y. Y.
623 performed bioinformatics and statistical analysis with help from J.L., and carried out
624 aCGH and qPCR experiments. G.X provided samples. G.Y. and L.Q. drafted the
625 manuscript. N.Y. revised the paper. All authors read and approved the final
626 manuscript.

627 **Competing interests**

628 The authors declare that they have no competing interests.

629 **Figure legends**

630 **Figure 1. The length and frequency distribution of CNVRs.** (A) Most CNVRs are
631 shorter than 10 kb. (B) 6,160 CNVRs (68.30%) events occur in only one individual.

632 **Figure 2. Correlation between digital aCGH and whole genome aCGH among**
633 **Luxi Game and White Leghorn compared with Red Jungle Fowl (RJF).** Digital
634 aCGH are estimated using calculated \log_2 CN ratios in which CN are estimated for
635 identified CNVs segments of two individuals and divided by the corresponding CN of
636 RJF. RJF is selected as the reference sample in each aCGH experiment, and aCGH
637 values are defined as the average of all probes \log_2 ratio values in the same segments
638 of digital aCGH.

639 **Figure 3. Validation of CNVR412 by qPCR in another 16 chickens.** X-axis
640 represents all 16 samples and Y-axis represents normalized ratios (NR) estimated by
641 qPCR. NR around 2 indicates normal status (2 copies), NR around 0 or 1 indicates
642 loss status (0 copies or 1 copy), and NR around 3 or more indicates gain status (3 or
643 more copies).

644 **Figure 4. Read depth and digital aCGH predictions and whole-genome aCGH**
645 **validations near preselected genetic loci for 5 representative chicken genomes.**

646 The uppermost gene image is generated with the UCSC Genome Browser
647 (<http://genome.ucsc.edu/>) using galGal4 assembly. The track below the gene region is
648 depth of coverage for all 5 individual genomes. Red indicates regions of excess read
649 depth ($> \text{mean} + 3 \times \text{STDEV}$), whereas gray indicates intermediate read depth ($\text{mean} +$
650 $2 \times \text{STDEV} < x < \text{mean} + 3 \times \text{STDEV}$), and green indicates normal read depth

651 (mean \pm 2 \times STDEV). All read depth values based on 1 kb non-overlapping windows
652 are corrected by GC content. Whole-genome aCGH and digital aCGH values are
653 depicted as red-green histograms and correspond to a gain colored in green (> 0.5), a
654 loss colored in red ($< - 0.5$) and normal status colored in gray ($- 0.5 < x < 0.5$). **(A)**
655 Two previous reported CNVs (chr20: 11,111,401-11,238,900 and chr20:
656 11,651,801-11,822,900) associated with dermal hyperpigmentation. The DX and SK
657 genomes show two additional copies of these regions compared with RJF, and are
658 validated by whole-genome aCGH. **(B)** A higher copy number increase for the *SOCS2*
659 locus (chr1:44,764,280-44,765,955) is predicted in LX than in other individuals. **(C)**
660 The *POPDC3* gene (chr3:68,255,196-68,259,535) is predicted duplication only in
661 WL.

662 **Figure 5. Hierarchical clustered heatmaps of preselected genetic loci for 12**
663 **chicken genomes.** Every block in the heatmap indicates estimated CN values of 1 kb
664 non-overlapping windows in preselected region. These heatmaps are generated from
665 hierarchical cluster analysis using Pearson's correlation of the CN values. The colors
666 for each bar denote different copy number (CN). **(A)** DX and SK which are predicted
667 to be doubled within dermal hyperpigmentation loci are clustered together. **(B)**
668 Upstream and downstream of *SOCS2* locus reveals higher CN values in DX, TB and
669 WC especially LX. **(C)** WL shows specific expansion in *POPDC3* locus and is split
670 into a separate clade.

671

672 **Tables**

673 **Table 1. Summary statistics for sequencing and CNVs of 12 individuals**

Chicken abbreviation ^a	Numbers of mapped reads	Depth	Coverage (%)	Autosome reads per 5 kb window ^b	Autosome reads STDEV	Duplications	Deletions	Sequence covered (Mb)
BY	102,002,937	9.7	97.0	489.29	110.73	1,344	631	34.4
CS	85,383,494	8.2	96.9	409.93	101.42	1,166	686	27.3
DX	129,847,015	12.4	97.4	623.50	130.46	592	848	8.5
LX	105,152,881	10.0	97.3	503.82	112.74	935	844	12.1
RIR	102,464,756	9.8	97.3	490.96	108.21	643	684	8.9
RJF	105,517,587	10.1	97.2	504.23	113.52	729	641	10.1
SG	85,987,827	8.2	96.6	412.27	87.66	510	568	7.5
SK	95,322,371	9.1	97.1	457.21	100.61	806	692	12.7
TB	107,535,104	10.3	97.3	515.68	108.07	642	705	8.8
WC	119,116,969	11.4	97.4	572.35	121.39	750	803	10.2
WL	118,689,980	11.3	97.5	567.18	118.63	226	477	3.7
WR	130,307,416	12.4	97.6	625.01	132.32	242	508	3.5

674 ^aBY, Beijing You; CS, Cornish; DX, Dongxiang; LX, Luxi Game; RIR, Red Island Rhode; RJF,

675 Red Jungle Fowl; SG, Shouguang; SK, Silkie; TB, Tibetan; WC, Wenchang; WL, White Leghorn;

676 WR, White Plymouth Rock.

677 ^bThe number of reads per 5 kb windows after GC correction.

678 **Table 2. Top 25 copy number variable genes in 12 chicken genomes**

Gene name	RefSeq accession	Gene size (bp)	Gene copy number estimates per individual ^a											
			BY	CS	DX	LX	RIR	RJF	SG	SK	TB	WC	WL	WR
<i>LOC418424</i>	NM_001030786	7,212	2.8	3.5	2.4	4.3	4.0	3.2	6.3	4.6	8.5	3.1	2.6	2.0
<i>LOC425362</i>	NM_001277974	648	4.0	2.9	3.4	4.2	2.5	6.0	7.1	4.1	5.2	3.0	1.7	2.9
<i>C20H20ORF111</i>	NM_001029981	7,087	9.4	11.9	7.2	7.1	8.6	9.4	9.0	12.0	10.1	9.1	9.8	10.1
<i>LOC100859427</i>	NM_001277807	1,118	4.7	3.5	3.0	3.6	2.8	4.1	3.1	7.9	4.0	5.1	2.9	2.8
<i>SOCS2</i>	NM_204540	1,676	1.6	1.8	3.0	6.4	2.0	1.6	1.4	1.3	3.6	2.4	1.5	1.7
<i>GBP</i>	NM_204652	2,531	1.4	0.2	4.1	2.3	2.1	2.5	3.1	4.4	4.5	3.1	2.0	3.6
<i>PTRH2</i>	NM_001040413	1,161	1.6	3.2	1.1	1.3	3.6	1.8	1.4	1.2	5.1	3.2	1.5	1.9
<i>LOC426914</i>	NM_001277964	981	4.9	2.7	3.2	3.9	2.2	4.0	1.9	5.6	4.2	4.4	2.4	3.0
<i>PRSS2</i>	NM_205384	2,812	2.8	0.6	3.7	3.9	2.8	3.1	2.2	2.5	3.1	2.3	0.9	3.2
<i>LOC100859722</i>	NM_001277975	660	2.6	3.1	3.6	4.2	5.1	5.2	4.1	2.2	3.6	4.0	4.8	4.4
<i>LOC100859616</i>	NM_001277973	749	1.5	1.4	2.4	2.8	2.9	1.5	2.1	3.7	2.1	3.5	3.6	4.1
<i>CD8A</i>	NM_001048080	3,183	3.5	3.6	5.2	2.5	2.7	2.1	3.9	2.5	2.5	3.0	2.4	3.0
<i>LOC425137</i>	NM_001278080	5,930	3.0	3.7	2.9	1.9	3.8	2.6	1.7	3.4	3.2	4.9	2.9	2.5
<i>LOC431317</i>	NM_001277978	586	1.6	2.8	2.1	2.6	4.0	3.9	3.5	1.3	2.2	3.1	3.0	2.9
<i>SLMO2</i>	NM_001030866	4,953	2.3	2.0	4.0	2.2	2.1	2.4	2.1	4.5	2.5	2.2	2.0	1.9
<i>TUBB1</i>	NM_205445	5,018	2.7	2.3	4.2	2.2	2.1	1.9	2.1	4.4	2.2	2.5	2.1	1.9
<i>LIMS1</i>	NM_001001766	13,454	3.9	4.7	5.2	5.1	4.6	3.4	4.5	4.2	5.3	4.7	2.4	4.7
<i>LOC770639</i>	NM_001277770	734	2.5	2.8	3.1	3.7	3.8	1.5	3.7	2.7	3.2	4.0	2.9	4.4
<i>ZNF692</i>	NM_001099356	6,224	2.2	4.2	1.3	2.2	1.4	1.6	2.1	1.6	1.8	1.9	2.0	2.0
<i>RFT1</i>	NM_001142872	10,993	2.1	2.2	1.9	2.1	3.6	2.0	1.9	2.1	4.1	3.0	2.0	1.9
<i>LOC431316</i>	NM_001277972	741	1.6	2.3	1.4	1.9	3.7	2.8	2.4	1.4	2.2	3.2	3.0	2.1
<i>LOC693258</i>	NM_001044681	720	2.8	4.2	2.5	3.4	4.0	3.5	2.4	2.3	2.6	3.1	2.3	2.3
<i>LOC100859586</i>	NM_001277977	828	1.6	2.4	2.7	3.0	2.4	2.0	1.4	1.8	2.5	2.6	3.5	3.2
<i>SOX3</i>	NM_204195	1,823	1.0	2.4	1.5	2.0	2.5	3.2	2.7	1.9	1.6	1.9	2.2	3.1
<i>CD8A</i>	NM_205235	12,042	3.9	3.6	4.7	2.5	2.7	2.8	2.8	3.4	3.0	3.5	3.0	3.6

679 ^aBY, Beijing You; CS, Cornish; DX, Dongxiang; LX, Luxi Game; RIR, Red Island Rhode; RJF,

680 Red Jungle Fowl; SG, Shouguang; SK, Silkie; TB, Tibetan; WC, Wenchang; WL, White Leghorn;

681 WR, White Plymouth Rock.

682 **Supplementary figure legends**

683 **Supplementary Figure S1. Individualized chicken CNV map in the chicken**

684 **genome.** The horizontal black lines represent the draft chicken genome (UCSC
685 version galGal4). Tracks under the chromosomes indicate corresponding CNV status
686 of all individuals kept in the alphabetical order from top to bottom, for BY, CS, DX,
687 LX, RIR, RJF, SG, SK, TB, WC, WL and WR. Merged CNVRs from all individuals
688 are depicted above chromosomes. The colors for each bar denote different copy
689 number (CN) in CNV legend and different types of CNVRs. The downmost axis
690 shows the chromosomes and CNVs coordinate. Left-hand chromosomes are ordered
691 from left to right, and the right-hands are just reversed.

692 **Supplementary Figure S2. Correlation between digital aCGH and whole-genome**

693 **aCGH among nine individuals compared with Red Jungle Fowl (RJF).** Digital
694 aCGH are estimated using calculated \log_2 CN ratios in which CN are estimated for
695 identified CNVs segments of nine individuals and divided by the corresponding CN
696 of RJF. RJF is selected as the reference sample in each aCGH experiment, and aCGH
697 values are defined as the average of all probes \log_2 ratio values in the same segments
698 of digital aCGH.

699 **Supplementary Figure S3. Illustrating of qPCR confirmation results for three**

700 **selected CNVRs of different types.** X-axis represents all 12 samples and Y-axis
701 represents normalized ratios (NR) estimated by qPCR. NR around 2 indicates normal
702 status (2 copies), NR around 0 or 1 indicates loss status (0 copies or 1 copy), and NR
703 around 3 or more indicates gain status (3 or more copies). (A) Results for a gain status

704 of CNVR3598. **(B)** Results for a loss status of CNVR6710. **(C)** Results for a both
705 status of CNVR412.

706 **Supplementary Figure S4. Read depth and digital aCGH predictions and**
707 **whole-genome aCGH validations near preselected genetic loci for 12 chicken**
708 **genomes.** The uppermost gene image is generated with the UCSC Genome Browser
709 (<http://genome.ucsc.edu/>) using galGal4 assembly. The track below the gene region is
710 depth of coverage for all 12 individual genomes. Red indicates regions of excess read
711 depth ($> \text{mean} + 3 \times \text{STDEV}$), whereas gray indicates intermediate read depth ($\text{mean} +$
712 $2 \times \text{STDEV} < x < \text{mean} + 3 \times \text{STDEV}$), and green indicates normal read depth
713 ($\text{mean} \pm 2 \times \text{STDEV}$). All read depth values based on 1 kb non-overlapping windows
714 are corrected by GC content. Whole-genome aCGH and digital aCGH values are
715 depicted as red-green histograms and correspond to a gain colored in green (> 0.5), a
716 loss colored in red (< -0.5) and normal status colored in gray ($-0.5 < x < 0.5$). **(A)** Two
717 previous reported CNVs (chr20: 11,111,401-11,238,900 and chr20:
718 11,651,801-11,822,900) associated with dermal hyperpigmentation. The DX and SK
719 genomes show two additional copies of these regions compared with RJF, and are
720 validated by whole-genome aCGH. **(B)** A higher copy number increase for the *SOCS2*
721 locus (chr1:44,764,280-44,765,955) is predicted in LX than in other individuals. **(C)**
722 The *POPDC3* gene (chr3:68,255,196-68,259,535) is predicted duplication only in
723 WL.

724 **Supplementary tables**

725 **Supplementary Table S1. Summary of identified CNVs and CNVRs in 12**

726 **chicken genomes.**

727 **Supplementary Table S2. General statistics of the CNVRs on each chromosome.**

728 **Supplementary Table S3. Primers information and confirmation results of the 15**

729 **chosen CNVRs by qPCR analysis.**

730 **Supplementary Table S4. The detailed features of RefSeq genes completely or**

731 **partial overlapping with CNVRs.**

732 **Supplementary Table S5. Functional enrichment of GO and KEGG pathway**

733 **analysis of RefSeq genes covered by CNVRs.**

734 **Supplementary Table S6. The overlap information of QTLs and CNVRs across**

735 **the chicken genome.**

736 **References**

- 737 Abyzov A, Urban AE, Snyder M, Gerstein M. 2011. CNVnator: an approach to discover, genotype, and
738 characterize typical and atypical CNVs from family and population genome sequencing.
739 *Genome Res* **21**(6): 974-984.
- 740 Alkan C, Kidd JM, Marques-Bonet T, Aksay G, Antonacci F, Hormozdiari F, Kitzman JO, Baker C,
741 Malig M, Mutlu O et al. 2009. Personalized copy number and segmental duplication maps
742 using next-generation sequencing. *Nat Genet* **41**(10): 1061-1067.
- 743 Altshuler DM, Gibbs RA, Peltonen L, Dermitzakis E, Schaffner SF, Yu F, Bonnen PE, de Bakker PI,
744 Deloukas P, Gabriel SB et al. 2010. Integrating common and rare genetic variation in diverse
745 human populations. *Nature* **467**(7311): 52-58.
- 746 Andree B, Hillemann T, Kessler-Icekson G, Schmitt-John T, Jockusch H, Arnold HH, Brand T. 2000.
747 Isolation and characterization of the novel popeye gene family expressed in skeletal muscle
748 and heart. *Dev Biol* **223**(2): 371-382.
- 749 Bentley DR Balasubramanian S Swerdlow HP Smith GP Milton J Brown CG Hall KP Evers DJ Barnes
750 CL Bignell HR et al. 2008. Accurate whole human genome sequencing using reversible
751 terminator chemistry. *Nature* **456**(7218): 53-59.
- 752 Berglund J, Nevalainen EM, Molin AM, Perloski M, Andre C, Zody MC, Sharpe T, Hitte C,
753 Lindblad-Toh K, Lohi H et al. 2012. Novel origins of copy number variation in the dog
754 genome. *Genome Biol* **13**(8): R73.
- 755 Bickhart DM, Hou Y, Schroeder SG, Alkan C, Cardone MF, Matukumalli LK, Song J, Schnabel RD,
756 Ventura M, Taylor JF et al. 2012. Copy number variation of individual cattle genomes using
757 next-generation sequencing. *Genome Res* **22**(4): 778-790.
- 758 Brand T. 2005. The Popeye domain-containing gene family. *Cell Biochem Biophys* **43**(1): 95-103.
- 759 Burt DW. 2005. Chicken genome: current status and future opportunities. *Genome Res* **15**(12):
760 1692-1698.
- 761 Campbell CD, Sampas N, Tsalenko A, Sudmant PH, Kidd JM, Malig M, Vu TH, Vives L, Tsang P,
762 Bruhn L et al. 2011. Population-genetic properties of differentiated human copy-number
763 polymorphisms. *Am J Hum Genet* **88**(3): 317-332.
- 764 Chen K, Tu Y, Zhang Y, Blair HC, Zhang L, Wu C. 2008. PINCH-1 regulates the ERK-Bim pathway
765 and contributes to apoptosis resistance in cancer cells. *J Biol Chem* **283**(5): 2508-2517.
- 766 Connell S, Meade KG, Allan B, Lloyd AT, Downing T, O'Farrelly C, Bradley DG. 2013. Genome-wide
767 association analysis of avian resistance to *Campylobacter jejuni* colonization identifies risk
768 locus spanning the CDH13 gene. *G3 (Bethesda)* **3**(5): 881-890.
- 769 Conrad DF, Andrews TD, Carter NP, Hurler ME, Pritchard JK. 2006. A high-resolution survey of
770 deletion polymorphism in the human genome. *Nat Genet* **38**(1): 75-81.
- 771 Conrad DF, Pinto D, Redon R, Feuk L, Gokcumen O, Zhang Y, Aerts J, Andrews TD, Barnes C,
772 Campbell P et al. 2010. Origins and functional impact of copy number variation in the human
773 genome. *Nature* **464**(7289): 704-712.
- 774 Crooijmans RP, Fife MS, Fitzgerald TW, Strickland S, Cheng HH, Kaiser P, Redon R, Groenen MA.
775 2013. Large scale variation in DNA copy number in chicken breeds. *BMC Genomics* **14**: 398.
- 776 Dorshorst B, Molin AM, Rubin CJ, Johansson AM, Stromstedt L, Pham MH, Chen CF, Hallbook F,
777 Ashwell C, Andersson L. 2011. A complex genomic rearrangement involving the endothelin 3
778 locus causes dermal hyperpigmentation in the chicken. *PLoS Genet* **7**(12): e1002412.

- 779 Elferink MG, Vallee AA, Jungerius AP, Crooijmans RP, Groenen MA. 2008. Partial duplication of the
780 PRLR and SPEF2 genes at the late feathering locus in chicken. *BMC Genomics* **9**: 391.
- 781 Fan WL, Ng CS, Chen CF, Lu MY, Chen YH, Liu CJ, Wu SM, Chen CK, Chen JJ, Mao CT et al. 2013.
782 Genome-wide patterns of genetic variation in two domestic chickens. *Genome Biol Evol* **5**(7):
783 1376-1392.
- 784 Freeman JL, Perry GH, Feuk L, Redon R, McCarroll SA, Altshuler DM, Aburatani H, Jones KW,
785 Tyler-Smith C, Hurles ME et al. 2006. Copy number variation: new insights in genome
786 diversity. *Genome Res* **16**(8): 949-961.
- 787 Gokcumen O, Babb PL, Iskow RC, Zhu Q, Shi X, Mills RE, Ionita-Laza I, Vallender EJ, Clark AG,
788 Johnson WE et al. 2011. Refinement of primate copy number variation hotspots identifies
789 candidate genomic regions evolving under positive selection. *Genome Biol* **12**(5): R52.
- 790 Goto RM, Wang Y, Taylor RL, Jr., Wakenell PS, Hosomichi K, Shiina T, Blackmore CS, Briles WE,
791 Miller MM. 2009. BG1 has a major role in MHC-linked resistance to malignant lymphoma in
792 the chicken. *Proc Natl Acad Sci U S A* **106**(39): 16740-16745.
- 793 Greenwold MJ, Sawyer RH. 2010. Genomic organization and molecular phylogenies of the beta (beta)
794 keratin multigene family in the chicken (*Gallus gallus*) and zebra finch (*Taeniopygia guttata*):
795 implications for feather evolution. *BMC Evol Biol* **10**: 148.
- 796 Griffin DK, Robertson LB, Tempest HG, Vignal A, Fillon V, Crooijmans RP, Groenen MA, Deryusheva
797 S, Gaginskaya E, Carre W et al. 2008. Whole genome comparative studies between chicken
798 and turkey and their implications for avian genome evolution. *BMC Genomics* **9**: 168.
- 799 Hastings PJ, Ira G, Lupski JR. 2009. A microhomology-mediated break-induced replication model for
800 the origin of human copy number variation. *PLoS Genet* **5**(1): e1000327.
- 801 Henrichsen CN, Chaignat E, Reymond A. 2009. Copy number variants, diseases and gene expression.
802 *Hum Mol Genet* **18**(R1): R1-8.
- 803 Hincke MT, Nys Y, Gautron J, Mann K, Rodriguez-Navarro AB, McKee MD. 2012. The eggshell:
804 structure, composition and mineralization. *Front Biosci (Landmark Ed)* **17**: 1266-1280.
- 805 Hu ZL, Park CA, Wu XL, Reecy JM. 2013. Animal QTLdb: an improved database tool for livestock
806 animal QTL/association data dissemination in the post-genome era. *Nucleic Acids Res*
807 **41**(Database issue): D871-879.
- 808 Huang da W, Sherman BT, Lempicki RA. 2009. Systematic and integrative analysis of large gene lists
809 using DAVID bioinformatics resources. *Nat Protoc* **4**(1): 44-57.
- 810 Hytonen VP, Maatta JA, Kidron H, Halling KK, Horha J, Kulomaa T, Nyholm TK, Johnson MS,
811 Salminen TA, Kulomaa MS et al. 2005. Avidin related protein 2 shows unique structural and
812 functional features among the avidin protein family. *BMC Biotechnol* **5**: 28.
- 813 International Chicken Genome Sequencing Consortium. 2004. Sequence and comparative analysis of
814 the chicken genome provide unique perspectives on vertebrate evolution. *Nature* **432**(7018):
815 695-716.
- 816 Jia X, Chen S, Zhou H, Li D, Liu W, Yang N. 2013. Copy number variations identified in the chicken
817 using a 60K SNP BeadChip. *Anim Genet* **44**(3): 276-284.
- 818 Jiang L, Jiang J, Yang J, Liu X, Wang J, Wang H, Ding X, Liu J, Zhang Q. 2013. Genome-wide
819 detection of copy number variations using high-density SNP genotyping platforms in
820 Holsteins. *BMC Genomics* **14**: 131.
- 821 Karolchik D, Kuhn RM, Baertsch R, Barber GP, Clawson H, Diekhans M, Giardine B, Harte RA,
822 Hinrichs AS, Hsu F et al. 2008. The UCSC Genome Browser Database: 2008 update. *Nucleic*

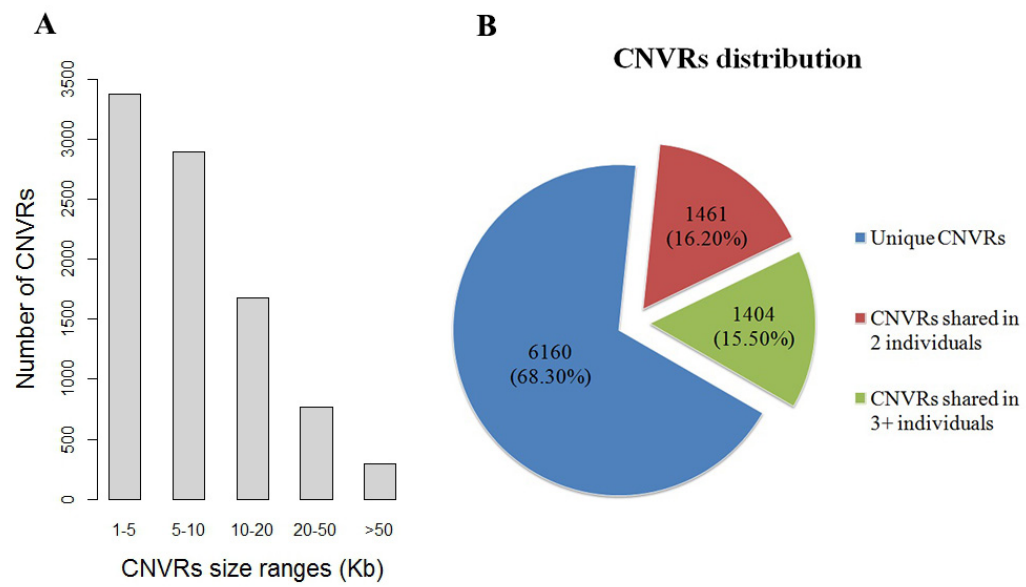
- 823 *Acids Res* **36**(Database issue): D773-779.
- 824 LaFramboise T. 2009. Single nucleotide polymorphism arrays: a decade of biological, computational
825 and technological advances. *Nucleic Acids Res* **37**(13): 4181-4193.
- 826 Lee C, Iafrate AJ, Brothman AR. 2007. Copy number variations and clinical cytogenetic diagnosis of
827 constitutional disorders. *Nat Genet* **39**(7 Suppl): S48-54.
- 828 Li H, Durbin R. 2009. Fast and accurate short read alignment with Burrows-Wheeler transform.
829 *Bioinformatics* **25**(14): 1754-1760.
- 830 Li H, Handsaker B, Wysoker A, Fennell T, Ruan J, Homer N, Marth G, Abecasis G, Durbin R. 2009.
831 The Sequence Alignment/Map format and SAMtools. *Bioinformatics* **25**(16): 2078-2079.
- 832 Liaw HJ, Chen WR, Huang YC, Tsai CW, Chang KC, Kuo CL. 2007. Genomic organization of the
833 chicken CD8 locus reveals a novel family of immunoreceptor genes. *J Immunol* **178**(5):
834 3023-3030.
- 835 Liu GE, Bickhart DM. 2012. Copy number variation in the cattle genome. *Funct Integr Genomics*
836 **12**(4): 609-624.
- 837 Liu GE, Hou Y, Zhu B, Cardone MF, Jiang L, Cellamare A, Mitra A, Alexander LJ, Coutinho LL,
838 Dell'Aquila ME et al. 2010. Analysis of copy number variations among diverse cattle breeds.
839 *Genome Res* **20**(5): 693-703.
- 840 Lorentzon M, Greenhalgh CJ, Mohan S, Alexander WS, Ohlsson C. 2005. Reduced bone mineral
841 density in SOCS-2-deficient mice. *Pediatr Res* **57**(2): 223-226.
- 842 Luo J, Yu Y, Mitra A, Chang S, Zhang H, Liu G, Yang N, Song J. 2013. Genome-wide copy number
843 variant analysis in inbred chickens lines with different susceptibility to Marek's disease. *G3*
844 (*Bethesda*) **3**(2): 217-223.
- 845 Manolio TA, Collins FS, Cox NJ, Goldstein DB, Hindorff LA, Hunter DJ, McCarthy MI, Ramos EM,
846 Cardon LR, Chakravarti A et al. 2009. Finding the missing heritability of complex diseases.
847 *Nature* **461**(7265): 747-753.
- 848 Marquez-Quinones A, Mutch DM, Debard C, Wang P, Combes M, Roussel B, Holst C, Martinez JA,
849 Handjieva-Darlenska T, Kalouskova P et al. 2010. Adipose tissue transcriptome reflects
850 variations between subjects with continued weight loss and subjects regaining weight 6 mo
851 after caloric restriction independent of energy intake. *Am J Clin Nutr* **92**(4): 975-984.
- 852 McCarroll SA, Altshuler DM. 2007. Copy-number variation and association studies of human disease.
853 *Nat Genet* **39**(7 Suppl): S37-42.
- 854 Metcalf D, Greenhalgh CJ, Viney E, Willson TA, Starr R, Nicola NA, Hilton DJ, Alexander WS. 2000.
855 Gigantism in mice lacking suppressor of cytokine signalling-2. *Nature* **405**(6790): 1069-1073.
- 856 Munoz-Amatriain M, Eichten SR, Wicker T, Richmond TA, Mascher M, Steuernagel B, Scholz U,
857 Ariyadasa R, Spannagl M, Nussbaumer T et al. 2013. Distribution, functional impact, and
858 origin mechanisms of copy number variation in the barley genome. *Genome Biol* **14**(6): R58.
- 859 Murai A, Furuse M, Kitaguchi K, Kusumoto K, Nakanishi Y, Kobayashi M, Horio F. 2009.
860 Characterization of critical factors influencing gene expression of two types of fatty
861 acid-binding proteins (L-FABP and Lb-FABP) in the liver of birds. *Comp Biochem Physiol A*
862 *Mol Integr Physiol* **154**(2): 216-223.
- 863 Nguyen DQ, Webber C, Ponting CP. 2006. Bias of selection on human copy-number variants. *PLoS*
864 *Genet* **2**(2): e20.
- 865 Nicholas TJ, Cheng Z, Ventura M, Mealey K, Eichler EE, Akey JM. 2009. The genomic architecture of
866 segmental duplications and associated copy number variants in dogs. *Genome Res* **19**(3):

- 867 491-499.
- 868 Norris BJ, Whan VA. 2008. A gene duplication affecting expression of the ovine ASIP gene is
869 responsible for white and black sheep. *Genome Res* **18**(8): 1282-1293.
- 870 Patel RK, Jain M. 2012. NGS QC Toolkit: a toolkit for quality control of next generation sequencing
871 data. *PLoS One* **7**(2): e30619.
- 872 Pinto D, Darvishi K, Shi X, Rajan D, Rigler D, Fitzgerald T, Lionel AC, Thiruvahindrapuram B,
873 Macdonald JR, Mills R et al. 2011. Comprehensive assessment of array-based platforms and
874 calling algorithms for detection of copy number variants. *Nat Biotechnol* **29**(6): 512-520.
- 875 Qu L, Li X, Xu G, Chen K, Yang H, Zhang L, Wu G, Hou Z, Yang N. 2006. Evaluation of genetic
876 diversity in Chinese indigenous chicken breeds using microsatellite markers. *Sci China C Life*
877 *Sci* **49**(4): 332-341.
- 878 Redon R, Ishikawa S, Fitch KR, Feuk L, Perry GH, Andrews TD, Fiegler H, Shaperro MH, Carson AR,
879 Chen W et al. 2006. Global variation in copy number in the human genome. *Nature* **444**(7118):
880 444-454.
- 881 Rosengren Pielberg G, Golovko A, Sundstrom E, Curik I, Lennartsson J, Seltenhammer MH, Druml T,
882 Binns M, Fitzsimmons C, Lindgren G et al. 2008. A cis-acting regulatory mutation causes
883 premature hair graying and susceptibility to melanoma in the horse. *Nat Genet* **40**(8):
884 1004-1009.
- 885 Sharp AJ, Locke DP, McGrath SD, Cheng Z, Bailey JA, Vallente RU, Pertz LM, Clark RA, Schwartz S,
886 Segraves R et al. 2005. Segmental duplications and copy-number variation in the human
887 genome. *Am J Hum Genet* **77**(1): 78-88.
- 888 Stranger BE, Forrest MS, Dunning M, Ingle CE, Beazley C, Thorne N, Redon R, Bird CP, de Grassi A,
889 Lee C et al. 2007. Relative impact of nucleotide and copy number variation on gene
890 expression phenotypes. *Science* **315**(5813): 848-853.
- 891 Sudmant PH, Kitzman JO, Antonacci F, Alkan C, Malig M, Tsalenko A, Sampas N, Bruhn L, Shendure
892 J, Eichler EE. 2010. Diversity of human copy number variation and multicopy genes. *Science*
893 **330**(6004): 641-646.
- 894 Szatkiewicz JP, Wang W, Sullivan PF, Sun W. 2013. Improving detection of copy-number variation by
895 simultaneous bias correction and read-depth segmentation. *Nucleic Acids Res* **41**(3):
896 1519-1532.
- 897 Teo SM, Pawitan Y, Ku CS, Chia KS, Salim A. 2012. Statistical challenges associated with detecting
898 copy number variations with next-generation sequencing. *Bioinformatics* **28**(21): 2711-2718.
- 899 Tian M, Wang Y, Gu X, Feng C, Fang S, Hu X, Li N. 2013. Copy number variants in locally raised
900 Chinese chicken genomes determined using array comparative genomic hybridization. *BMC*
901 *Genomics* **14**(1): 262.
- 902 Wang-Rodriguez J, Dreilinger AD, Alsharabi GM, Rearden A. 2002. The signaling adapter protein
903 PINCH is up-regulated in the stroma of common cancers, notably at invasive edges. *Cancer*
904 **95**(6): 1387-1395.
- 905 Wang J, Jiang J, Fu W, Jiang L, Ding X, Liu JF, Zhang Q. 2012a. A genome-wide detection of copy
906 number variations using SNP genotyping arrays in swine. *BMC Genomics* **13**: 273.
- 907 Wang X, Nahashon S, Feaster TK, Bohannon-Stewart A, Adefope N. 2010. An initial map of
908 chromosomal segmental copy number variations in the chicken. *BMC Genomics* **11**: 351.
- 909 Wang Y, Gu X, Feng C, Song C, Hu X, Li N. 2012b. A genome-wide survey of copy number variation
910 regions in various chicken breeds by array comparative genomic hybridization method. *Anim*

- 911 *Genet* **43**(3): 282-289.
- 912 Wapinski I, Pfeffer A, Friedman N, Regev A. 2007. Natural history and evolutionary principles of gene
913 duplication in fungi. *Nature* **449**(7158): 54-61.
- 914 Wong GK Liu B Wang J Zhang Y Yang X Zhang Z Meng Q Zhou J Li D Zhang J et al. 2004. A genetic
915 variation map for chicken with 2.8 million single-nucleotide polymorphisms. *Nature*
916 **432**(7018): 717-722.
- 917 Wright D, Boije H, Meadows JR, Bed'hom B, Gourichon D, Vieaud A, Tixier-Boichard M, Rubin CJ,
918 Imsland F, Hallbook F et al. 2009. Copy number variation in intron 1 of SOX5 causes the
919 Pea-comb phenotype in chickens. *PLoS Genet* **5**(6): e1000512.
- 920 Yalcin B, Wong K, Agam A, Goodson M, Keane TM, Gan X, Nellaker C, Goodstadt L, Nicod J,
921 Bhomra A et al. 2011. Sequence-based characterization of structural variation in the mouse
922 genome. *Nature* **477**(7364): 326-329.
- 923 Yoon S, Xuan Z, Makarov V, Ye K, Sebat J. 2009. Sensitive and accurate detection of copy number
924 variants using read depth of coverage. *Genome Res* **19**(9): 1586-1592.
- 925 Zhang F, Gu W, Hurles ME, Lupski JR. 2009. Copy number variation in human health, disease, and
926 evolution. *Annu Rev Genomics Hum Genet* **10**: 451-481.

927 **Figure 1**

928

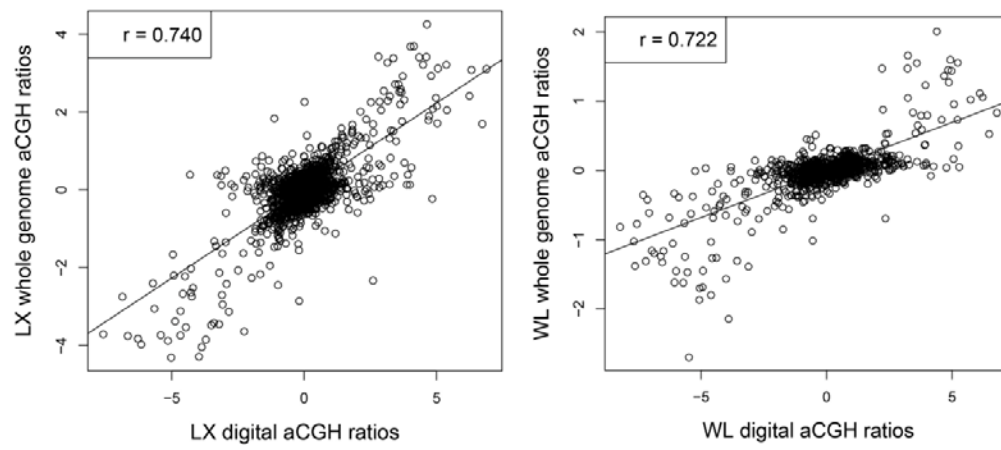


929

930

931 **Figure 2**

932

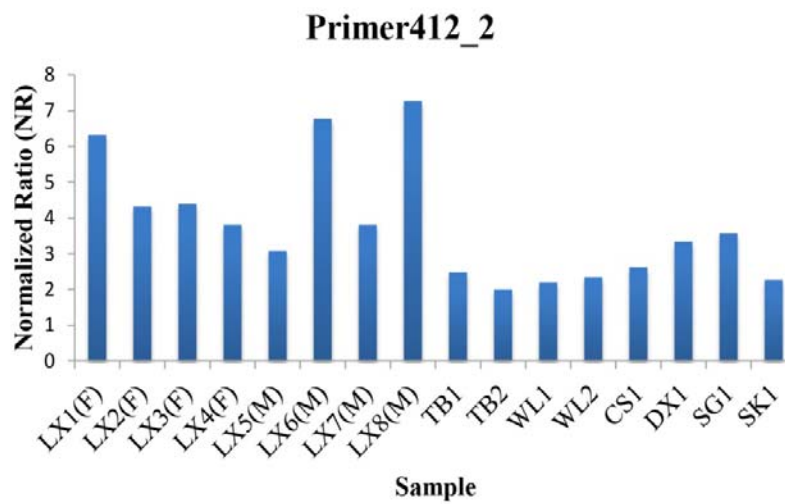


933

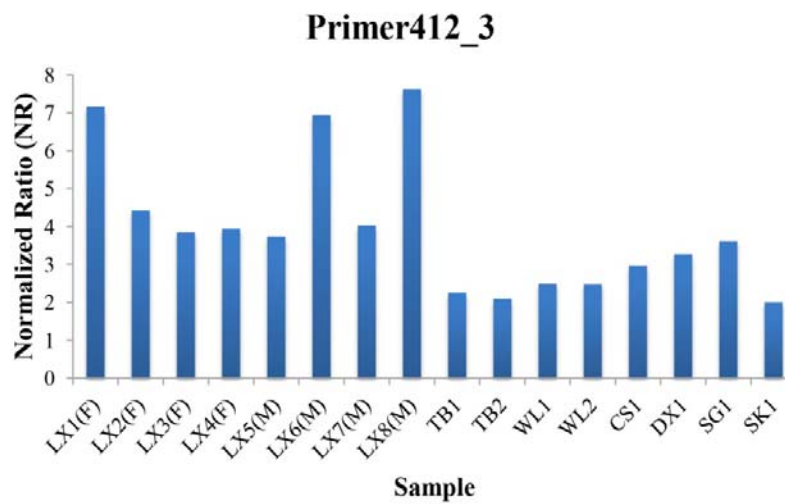
934

935 **Figure 3**
936

A

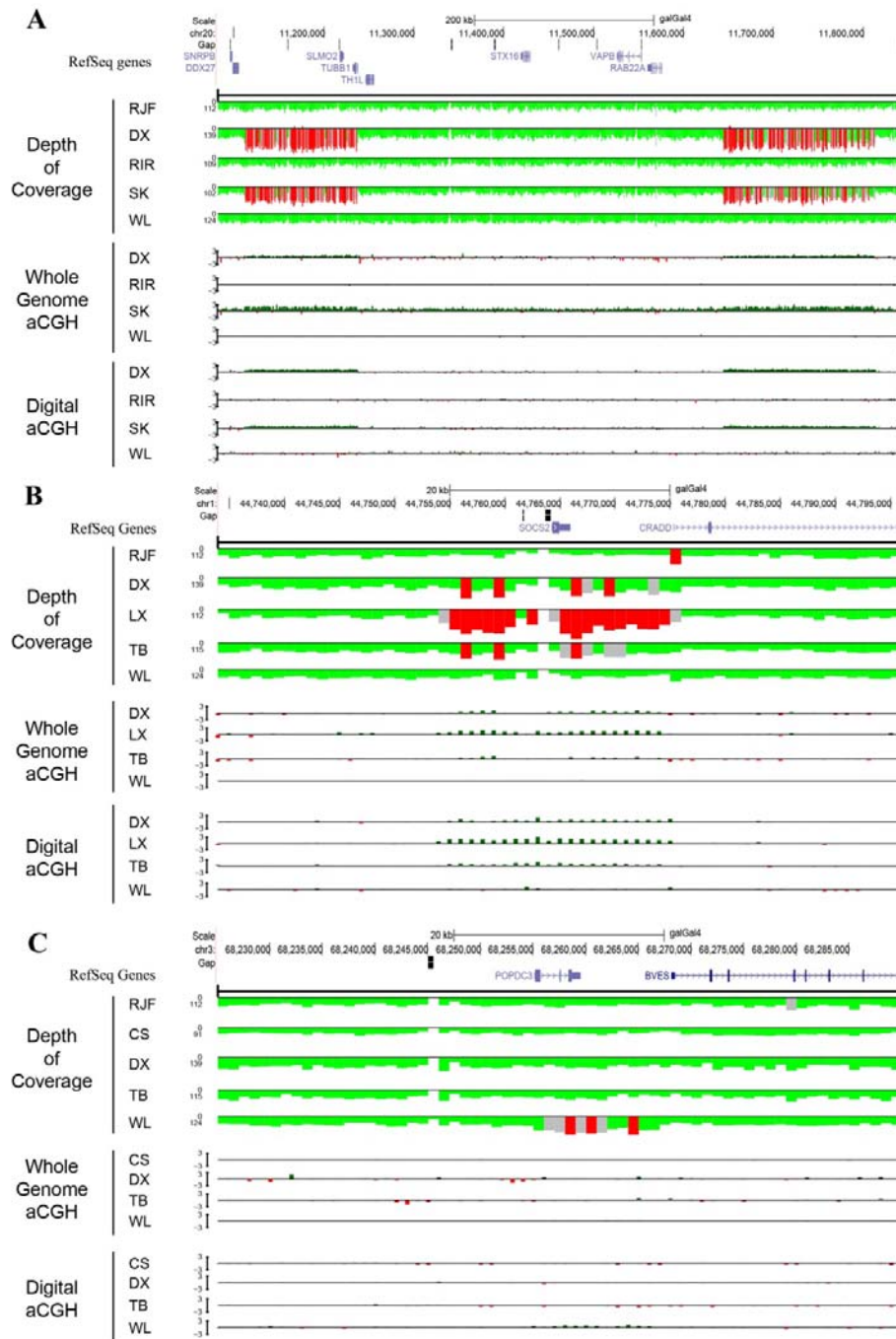


B



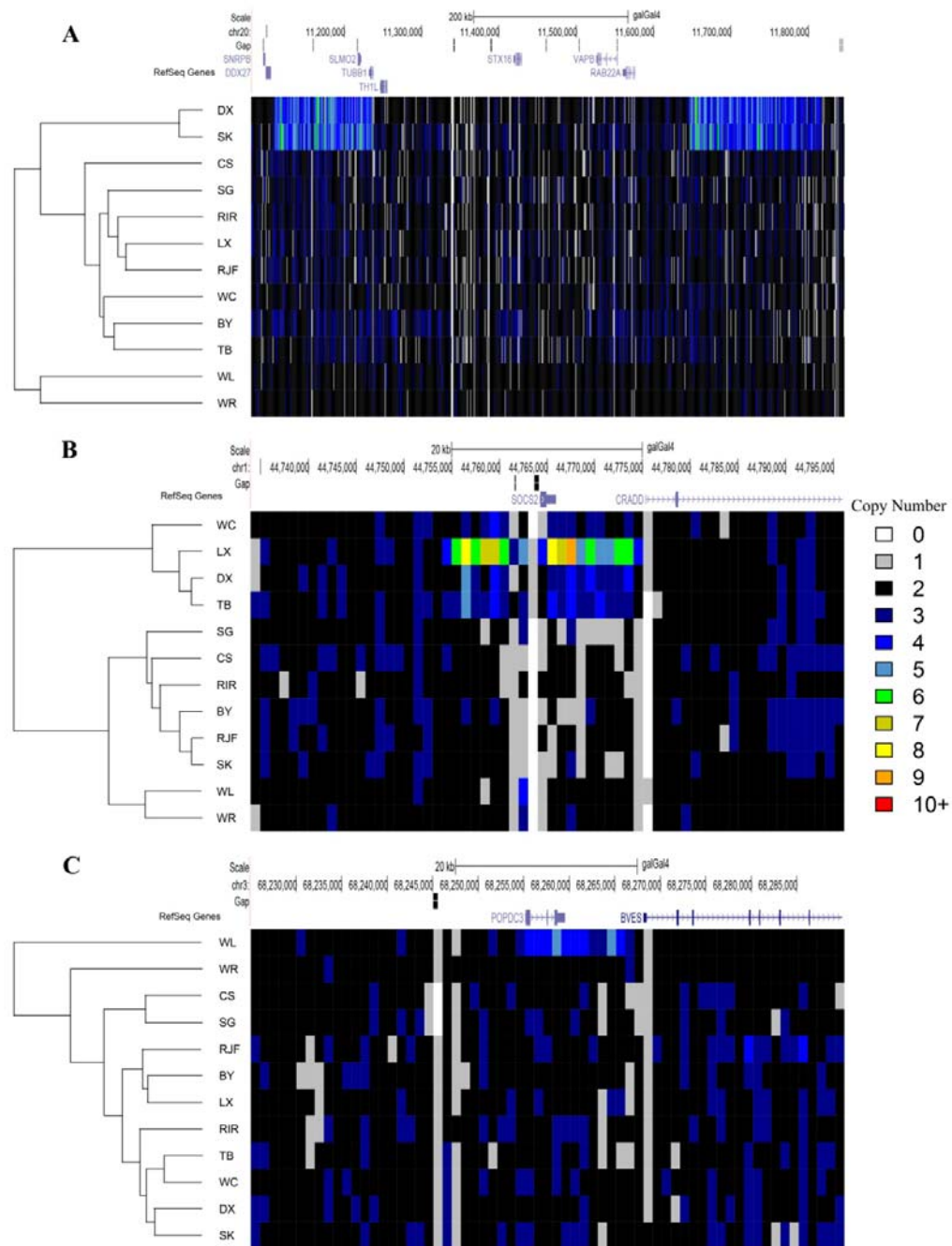
937

938 **Figure 4**
 939

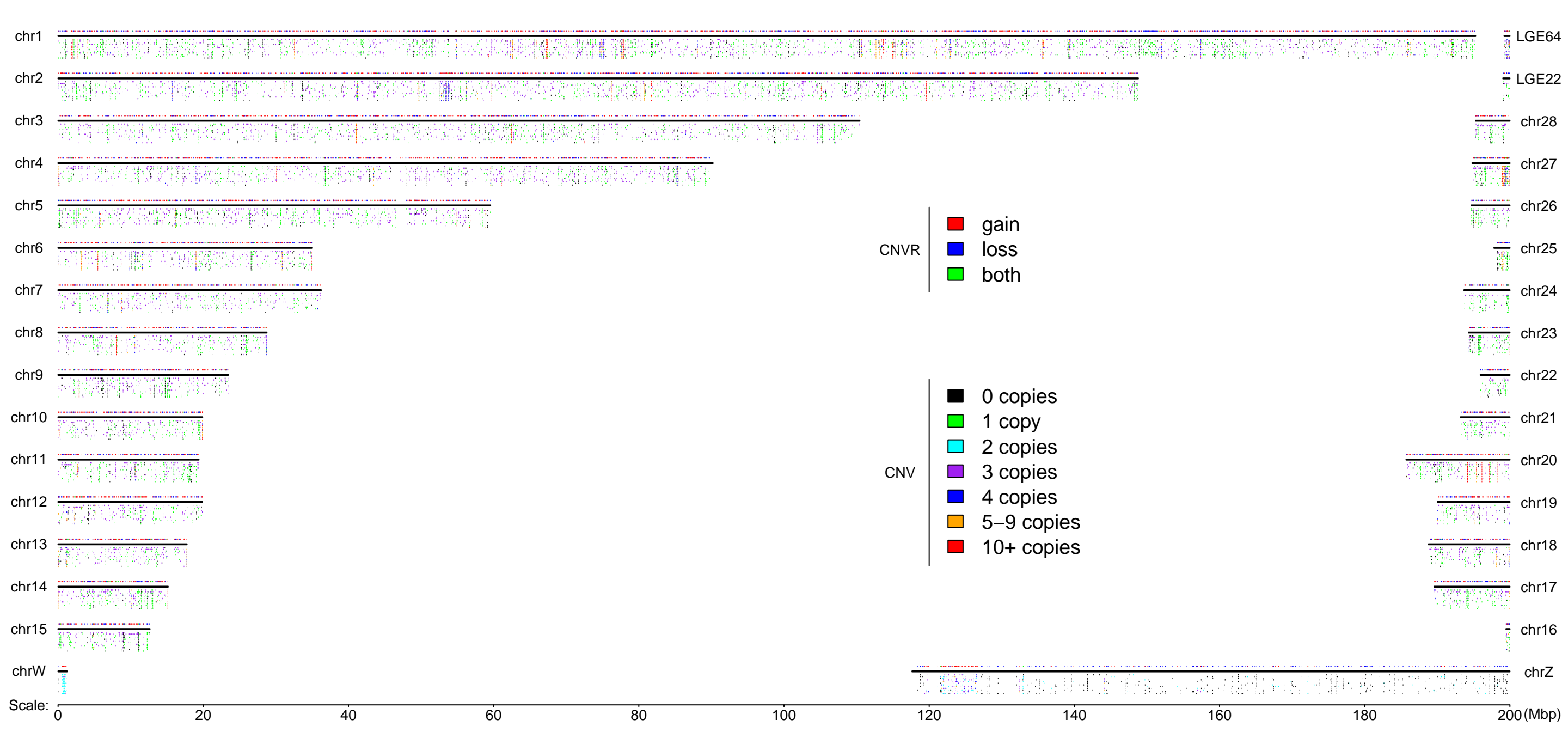


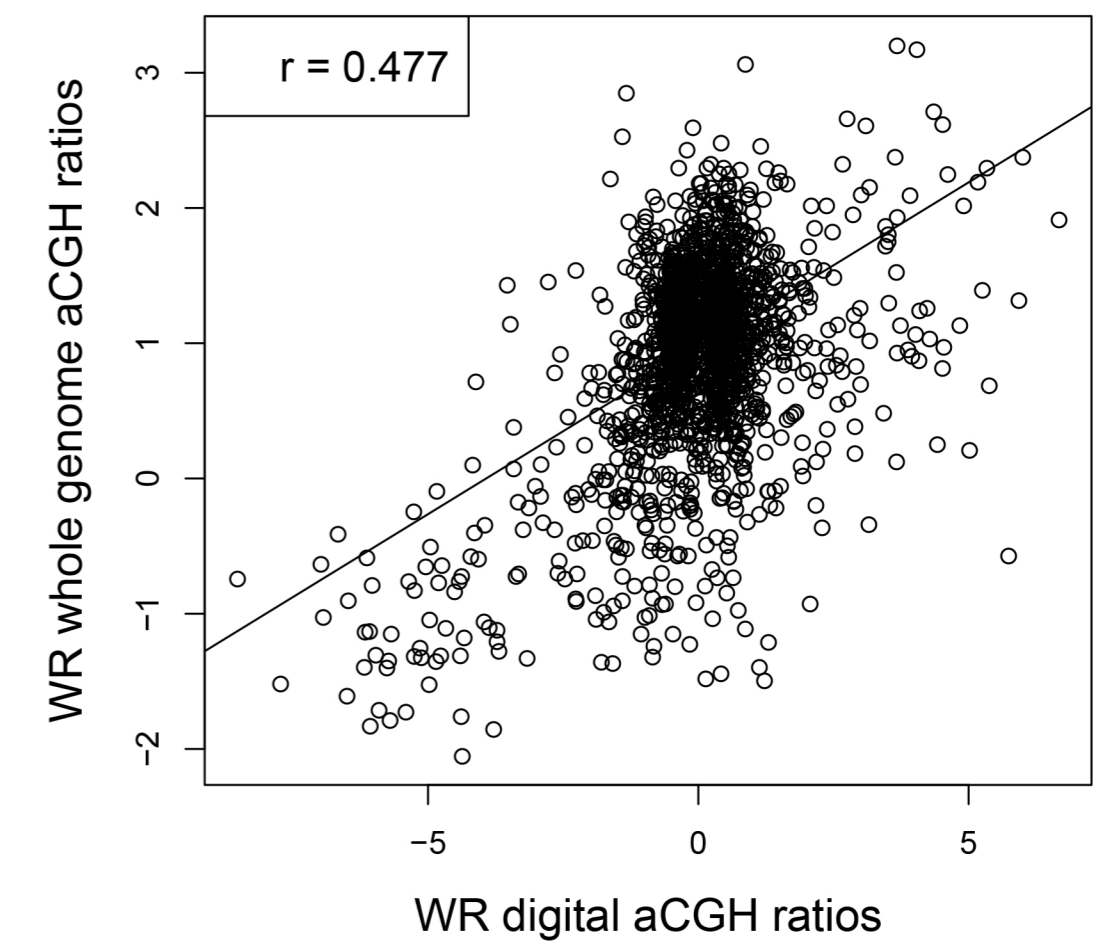
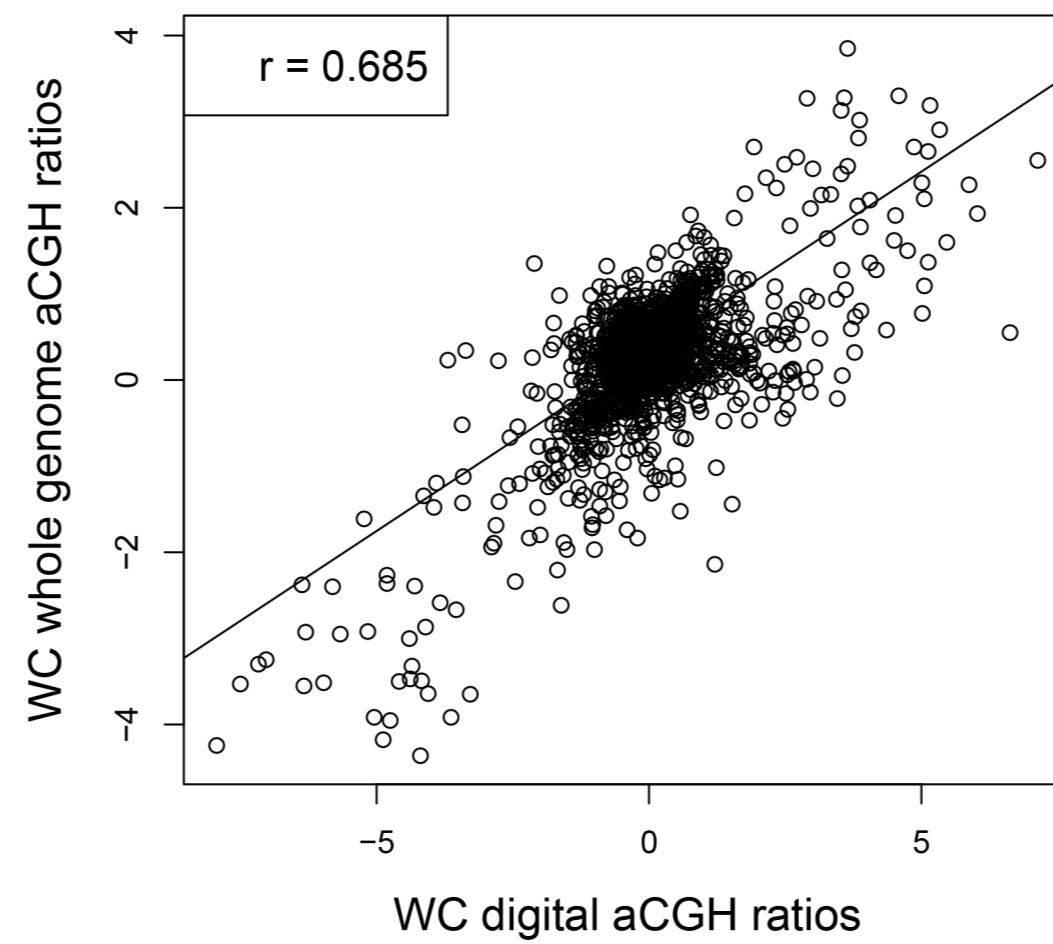
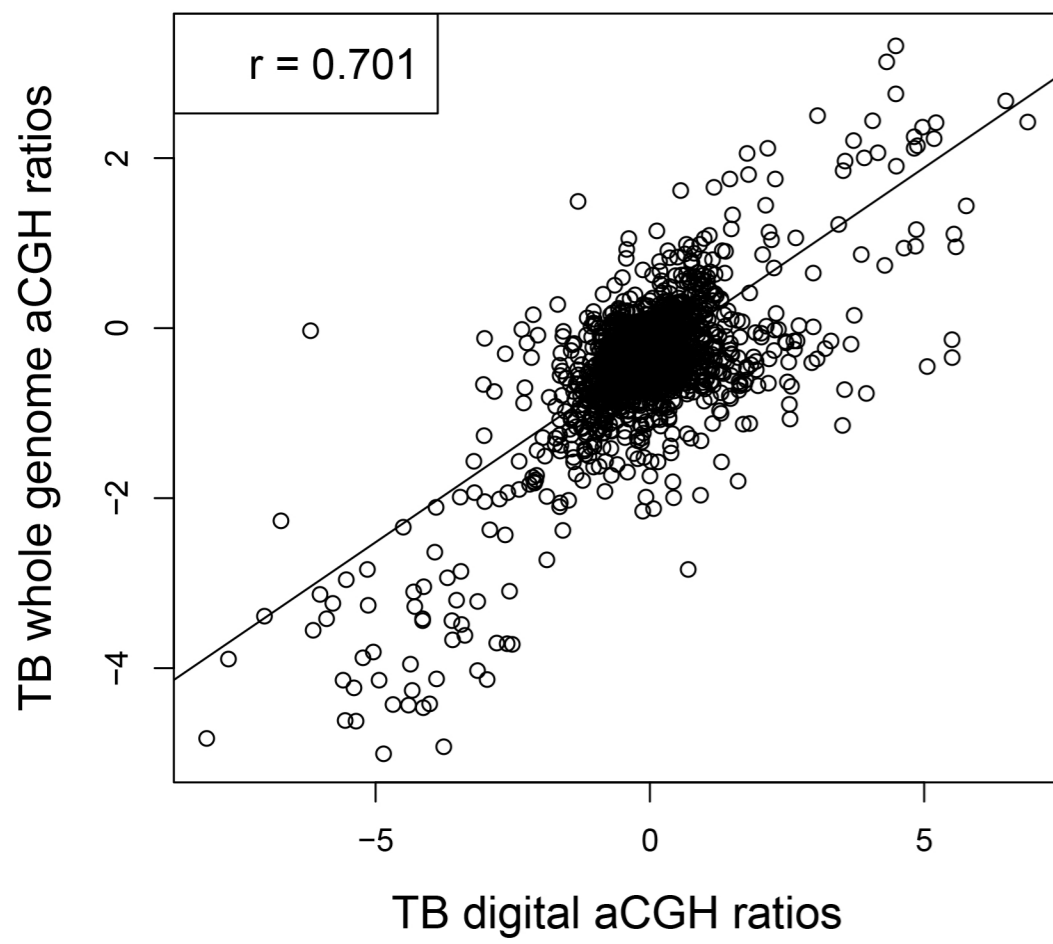
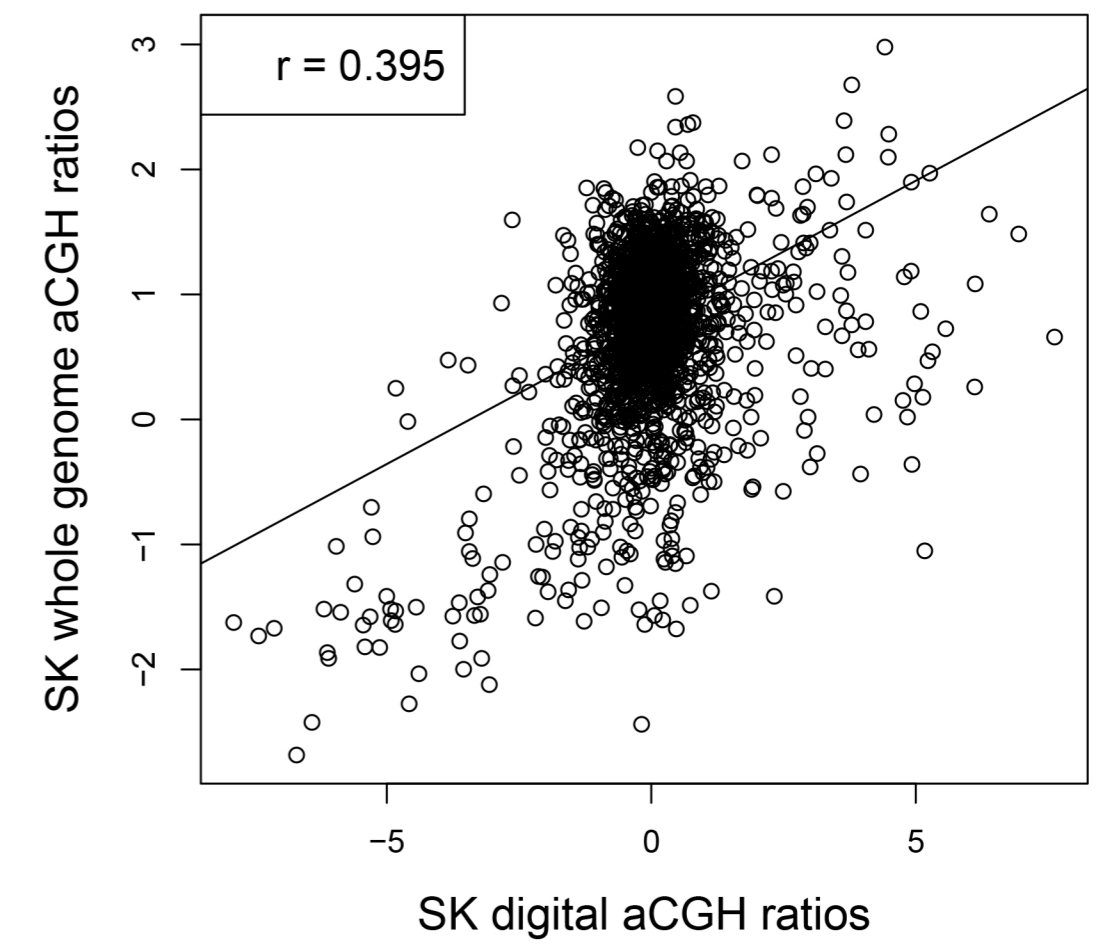
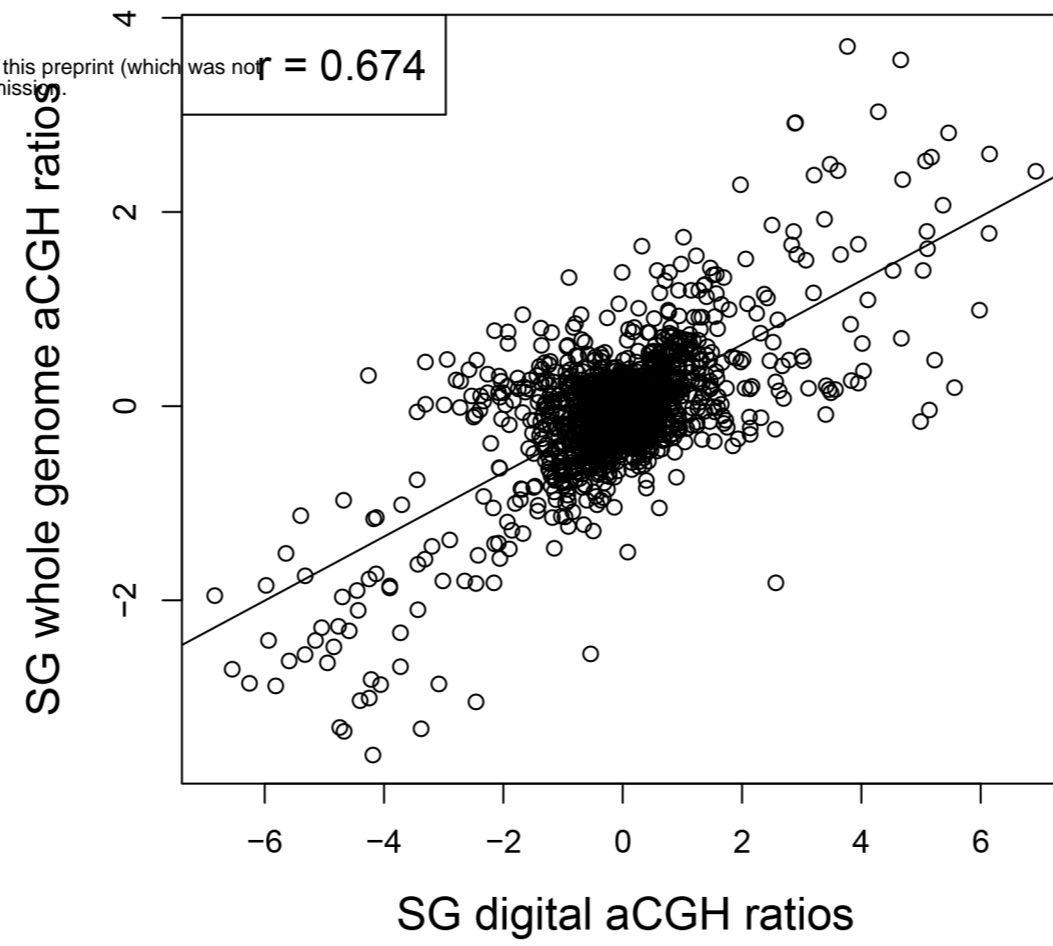
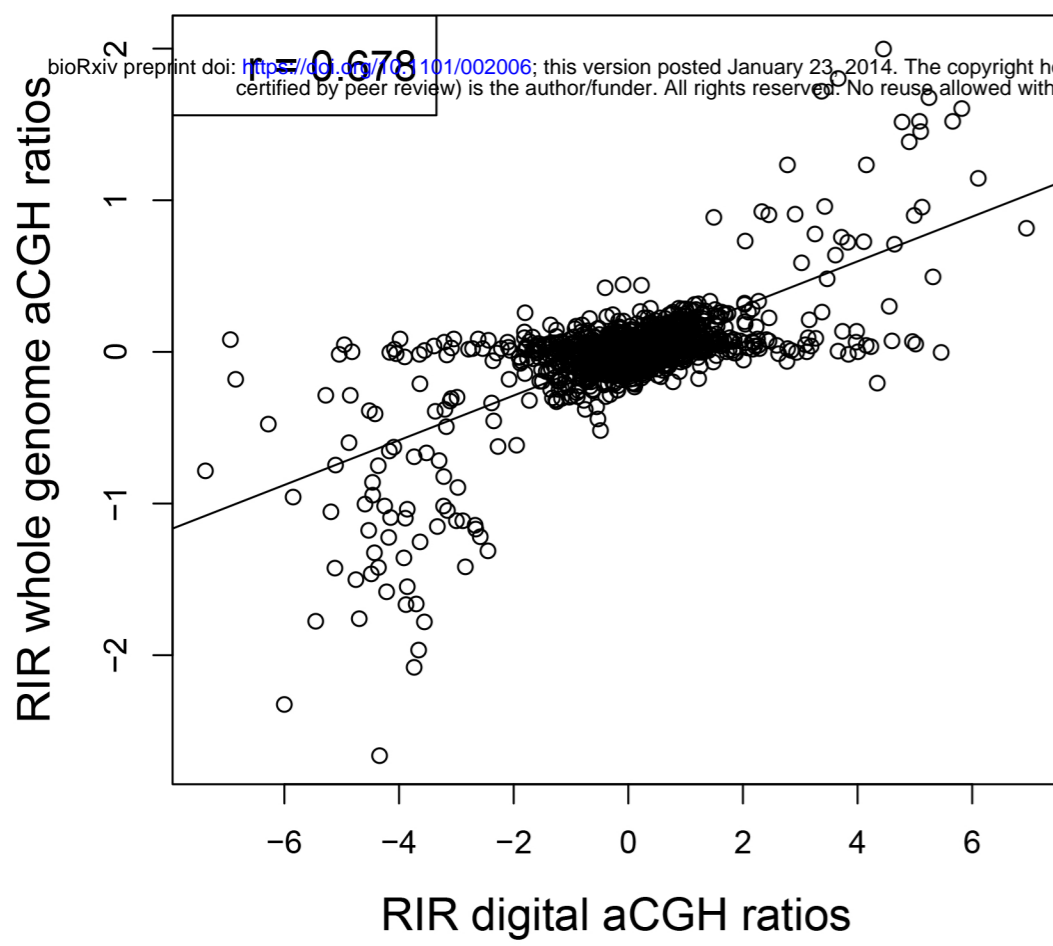
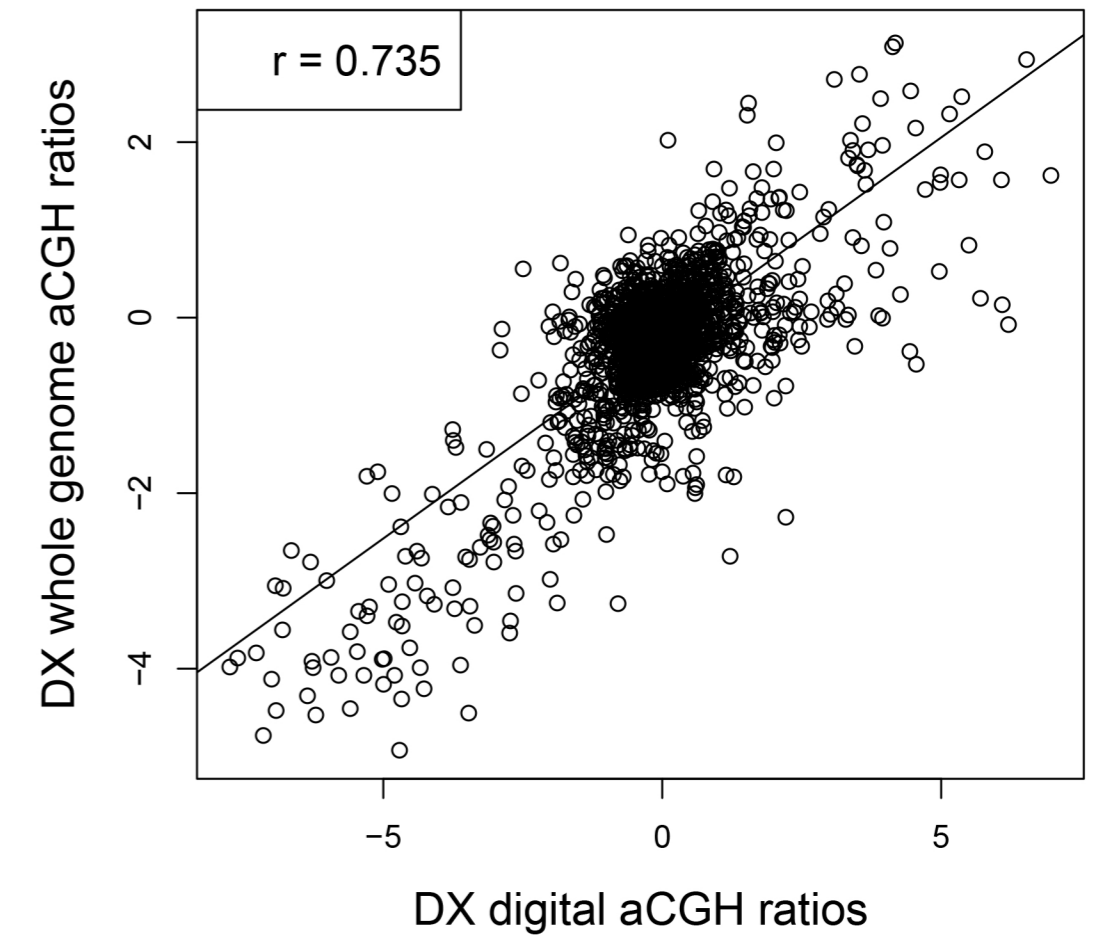
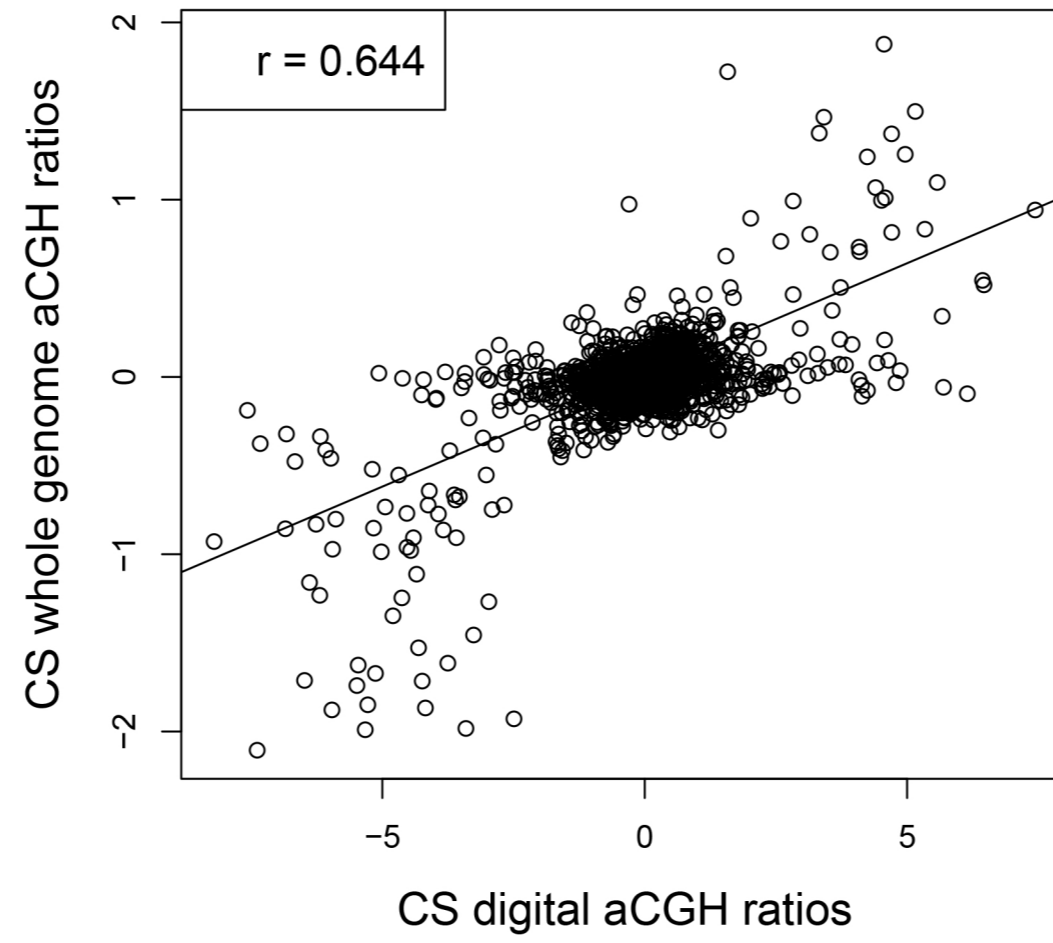
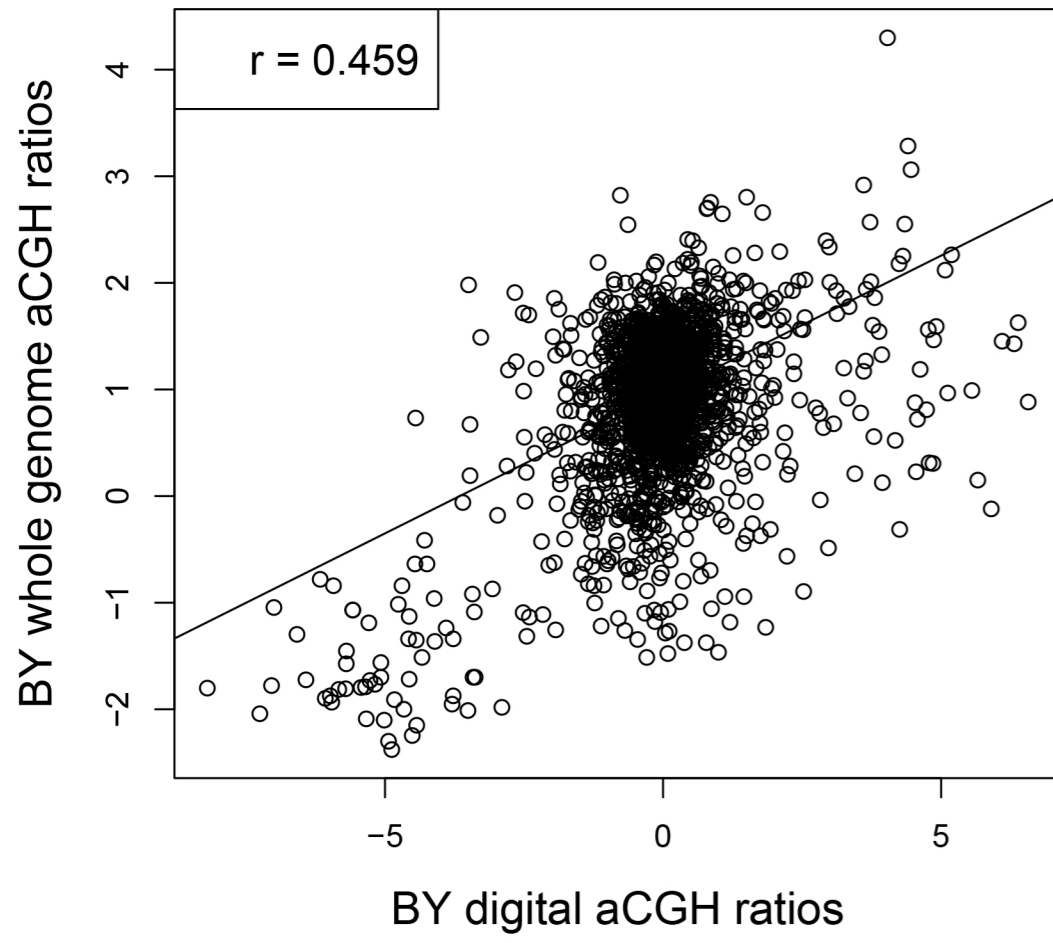
940

941 **Figure 5**
942

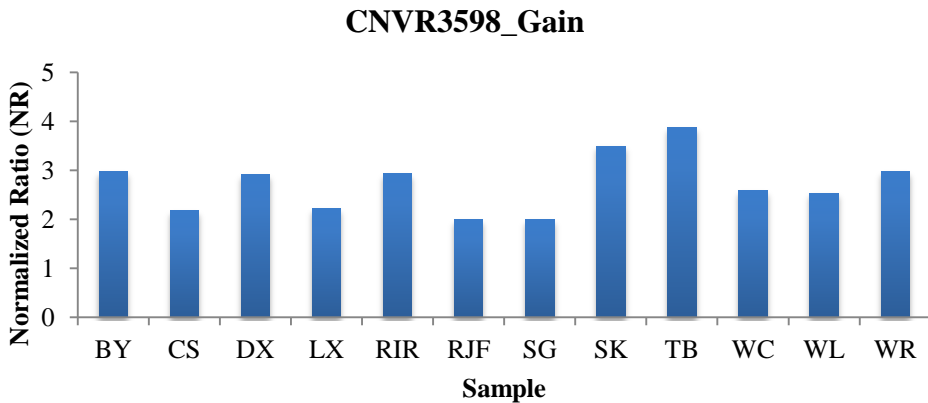


943

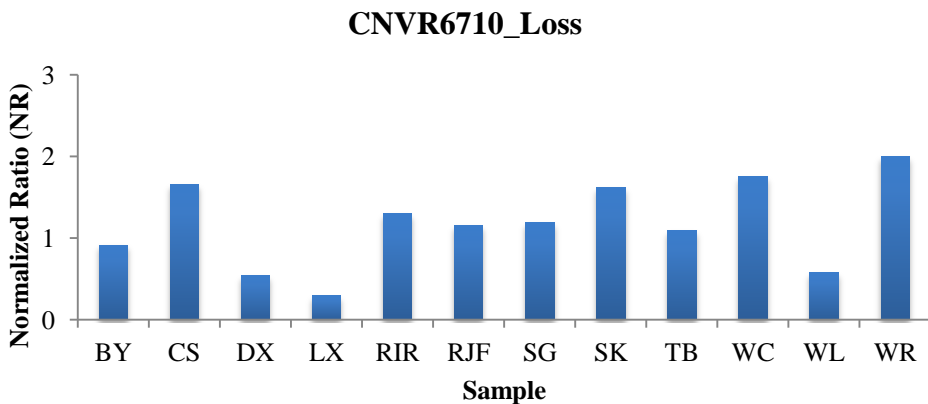




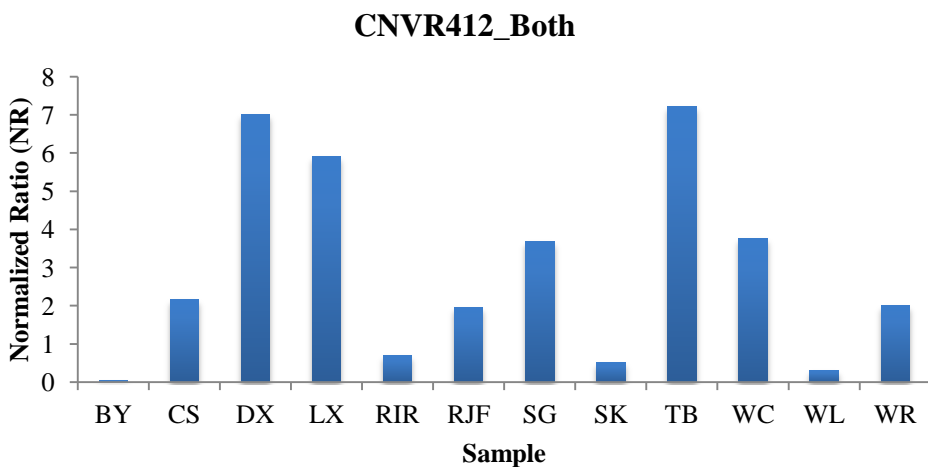
A

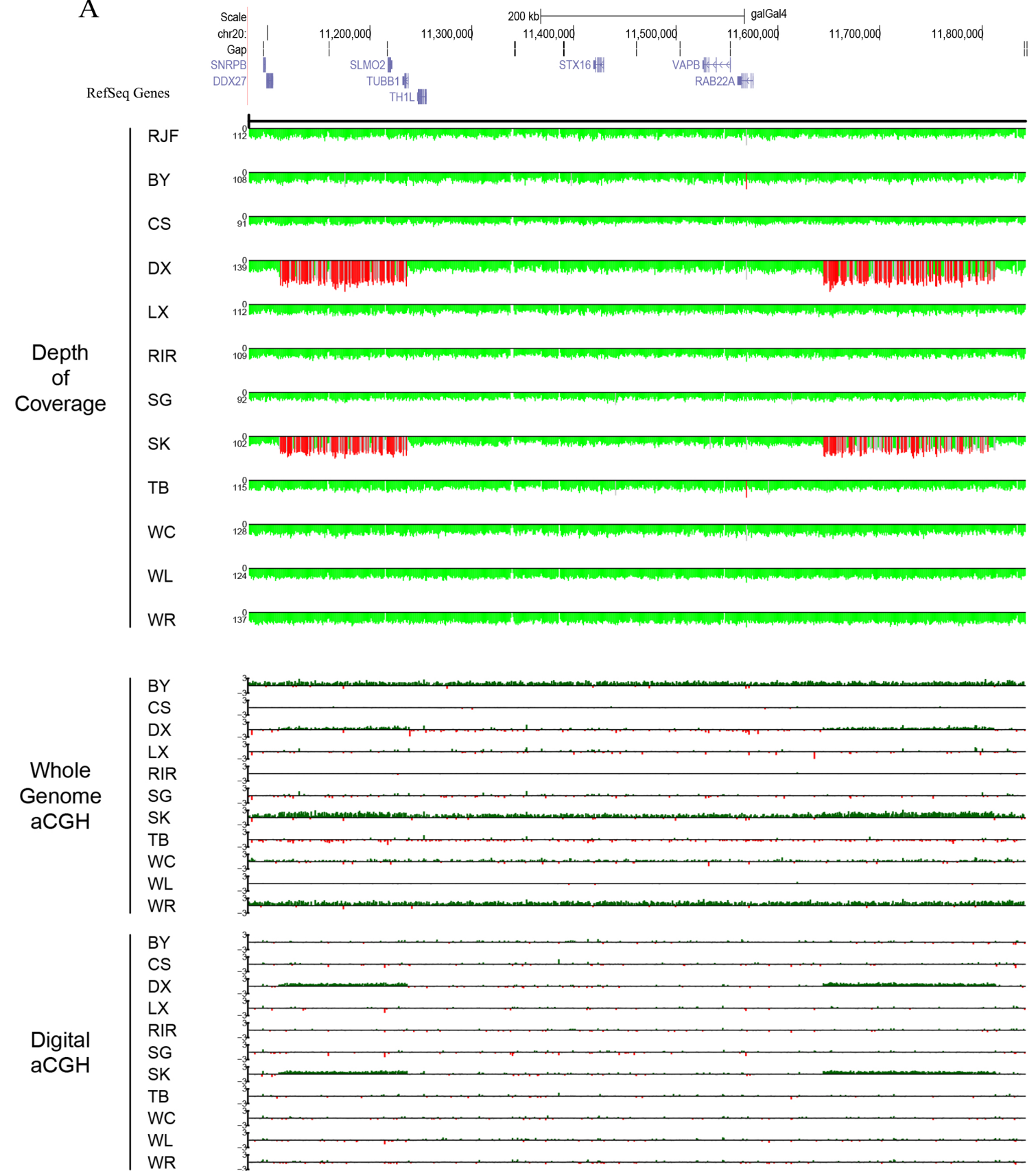
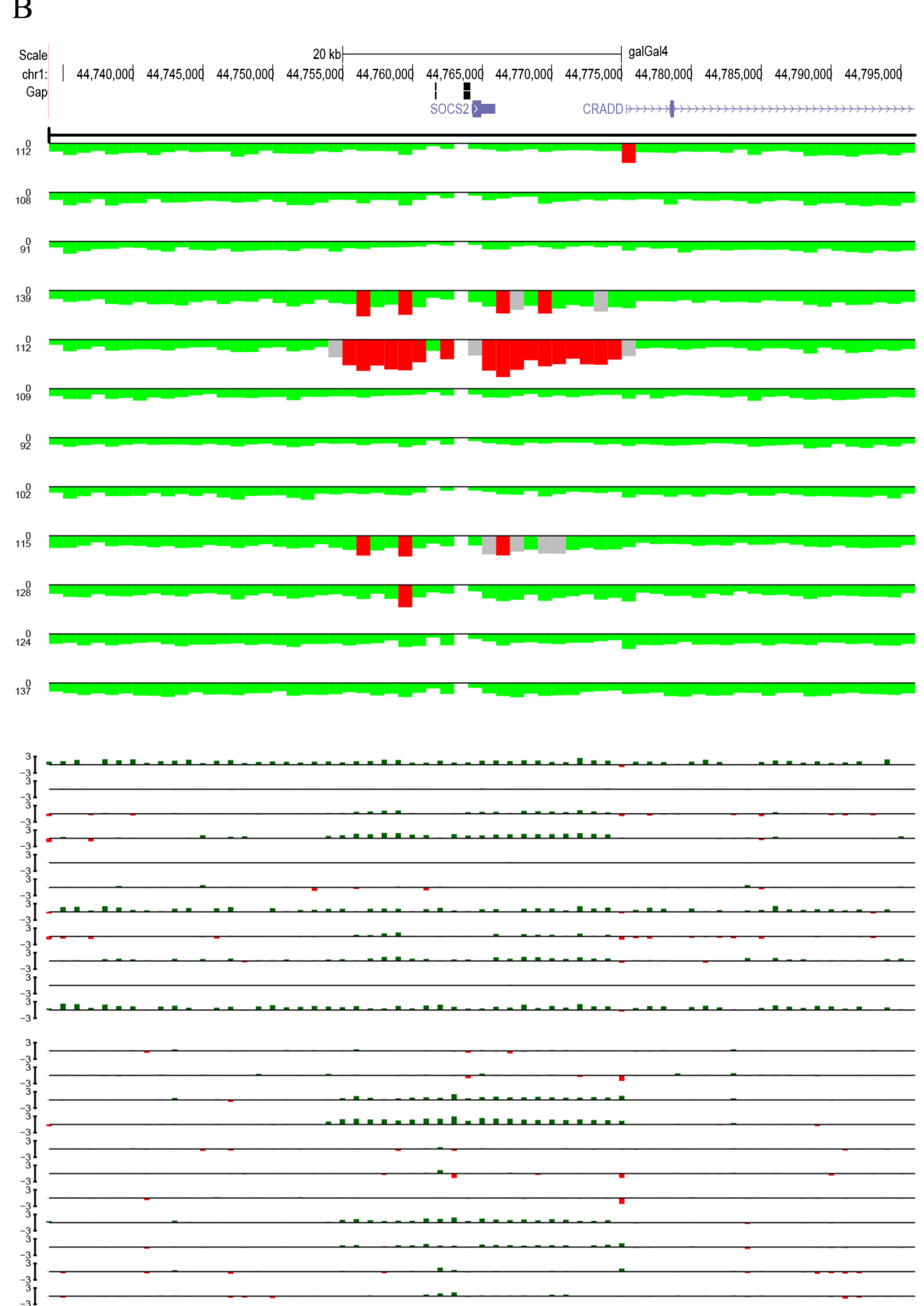


B



C



A**B****C**